Dalton Transactions

Accepted Manuscript

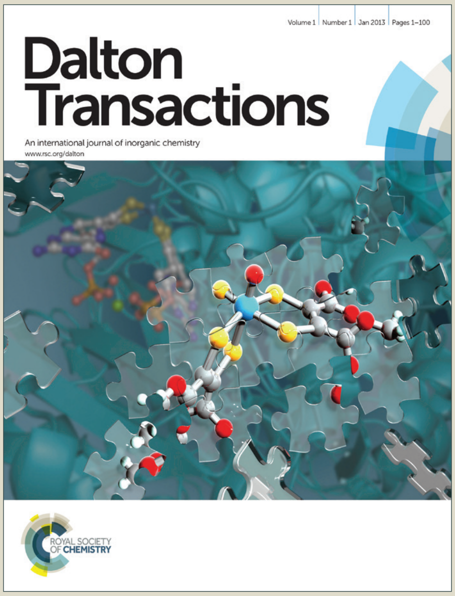

Graphical Abstract

Fundamental chemistry of iodine. The reaction of di-iodine towards thiourea and its methyl-derivative; formation of aminothiazoles and aminothiadiazoles through dicationic disulfides.

M. Biesiada, N. Kourkoumelis, M. Kubicki, A. Owczarzak, V. Balas, S.K. Hadjikakou

The reactivity of di-iodine towards thiourea (TU) and its derivative methylthiourea (MeTU) is studied. A diversity of products was obtained from these reactions which includes compounds of dicationic disulfides as counterparts; $[(TU_2)^{2+}\ 2(I^-)\cdot H_2O]$ (**1**), $[2(TU_2)^{2+}\cdot(Cl^-)\cdot 2(I^-)\cdot(I_3^-)]$ (**2**), $[(TUH)^+ (I_3^-)]$ (**3**) $[(TU_2)^{2+} (Br^-) (I_3^-)]$ (**4**), $[(TU_2)^{2+}\ 2(Br^-)\cdot H_2O]$ (**5**) and $[2(MeTU_2)^{2+}\cdot(2Br^-)\cdot(I_4^{2-})]$ (**7**) and heterocyclic iocnic compounds; $[(DAThdH^+)(I^-)]$ (**6**) (DAThd=3,5-diamino-1,2,4-thiadiazole), $[(DMeAThH^+)(I^-)(H_2O)]$ (**8**). $[(AMeAThdH^+)(I_3^-)]$ (**9**) (AMeAThdH= 5-amino-3-methylamino-4-methyl-1,2,4-thiadiazolium).

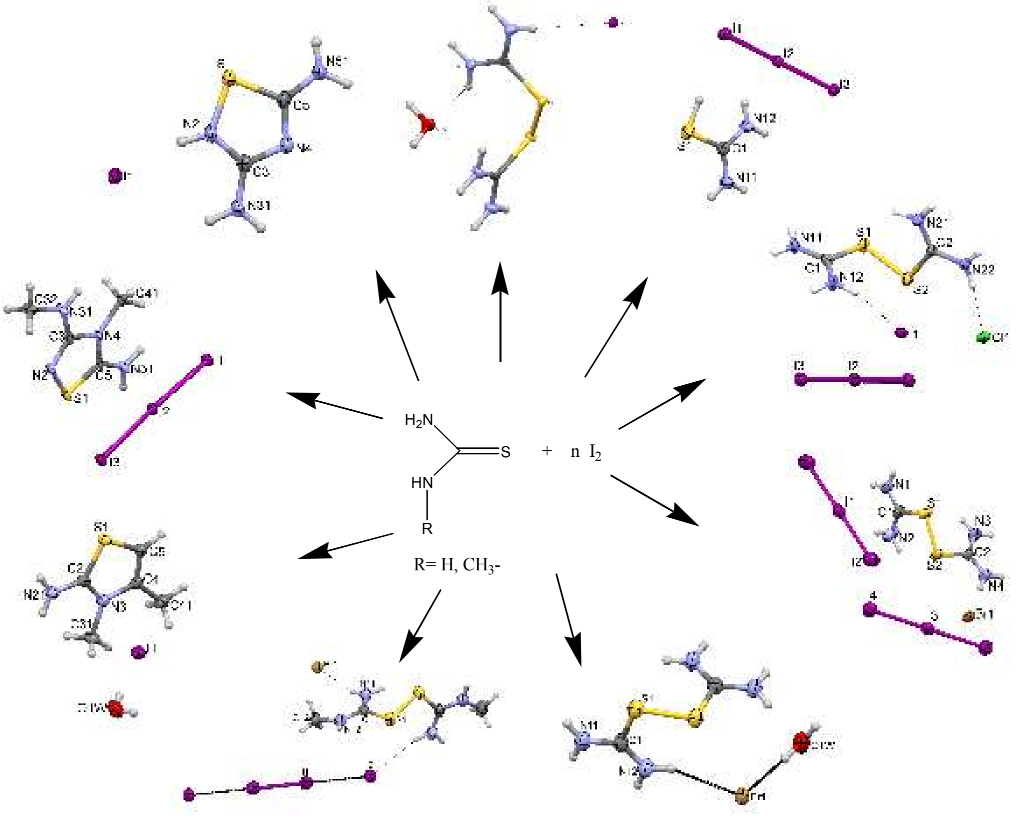

Fundamental chemistry of iodine. The reaction of di-iodine towards thiourea and its methyl-derivative; formation of aminothiazoles and aminothiadiazoles through dicationic disulfides.

M. Biesiada [a,b], N. Kourkoumelis[c], M. Kubicki*[b], A. Owczarzak[b], V. Balas[a], S.K. Hadjikakou[a]**

[a] Section of Inorganic and Analytical Chemistry, Department of Chemistry, University of Ioannina, 45110 Ioannina, Greece; [b] Department of Chemistry, A. Mickiewicz University, Umultowska 89b, 61-614 Poznań, Poland; [c] Medical Physics Laboratory, Medical School, University of Ioannina, Greece.

All correspondence should be addressed to:

* Dr M Kubicki: e-mail: mkubicki@amu.edu.pl; tel +48-618291256

** Professor Dr. S.K. Hadjikakou; e-mail: shadjika@uoi.gr; tel. xx30-26510-08374;

fax xx30-26510-08786

Abstract

The reactivity of di-iodine towards thiourea (TU) and its derivative methylthiourea (MeTU) is studied. A diversity of products was obtained from these reactions. TU reacts with di-iodine in the absence or presence of hydroiodic or hydrochloric acids in 1:1, 1:1:1 or 1:1:2 (TU:I_2:HX(X=I, Cl)) molar ratios to form the ionic compounds $[(TU_2)^{2+} 2(I^-)\cdot H_2O]$ (**1**), $[2(TU_2)^{2+}\cdot(Cl^-)\cdot 2(I^-)\cdot(I_3^-)]$ (**2**) and $[(TUH)^+ (I_3^-)]$ (**3**). The compounds $[(TU_2)^{2+} (Br^-) (I_3^-)]$ (**4**) and $[(TU_2)^{2+} 2(Br^-)\cdot H_2O]$ (**5**) were derived from the reactions of TU with di-iodine in the presence of hydrobromic acid in 1:1:1 or 1:2:1 (TU:I_2:HBr) molar ratios. However, when the product of the reaction between TU and di-iodine in 2:1 (TU:I_2) molar ratio is crystallized in acetone/ethyl-ether media the ionic salt of formula $[(DAThdH^+)(I^-)]$ (**6**) (DAThd=3,5-diamino-1,2,4-thiadiazole) is obtained. Methylthiourea (MeTU) reacts with di-iodine in the presence of hydrobromic acid (1:1:1, MeTU:I_2:HBr) in dichloromethane to form a solid product which gives the $[2(MeTU_2)^{2+}\cdot(2Br^-)\cdot(I_4^{2-})]$ (**7**). Moreover, MeTU reacts with I_2 in 2:1 (MeTU:I_2) to form an intermediate powder product which was crystallized in acetone to give the 2-amino-3,4-dimethylthiazolium cation in $[(DMeAThH^+)(I^-)(H_2O)]$ (**8**). Upon changing of the crystallization media to ethanol, instead of acetone, the cationic 5-amino-3-methylamino-4-methyl-1,2,4-thiadiazolium $(AMeAThdH)^+$ in $[(AMeAThdH^+)(I_3^-)]$ (**9**) is formed. The compounds were characterized by m.p, FT-IR, UV-Vis, ^{1}H-NMR spectroscopy and mass spectrometry. The crystal structures of compounds **1-9** were determined by X-ray crystallography.

Keywords:

Iodine chemistry, charge transfer complexes, thiourea, methylthiourea aminothiazoles crystal structures.

Introduction

Direct reactions of di-iodine with thioamides are known to lead to a variety of products. These include~~:~~ Charge Transfer (CT) complexes known as “spoke structures” (LS-I_2) and “extended spoke structures” (LS-I_2-I_2) [1-9]. Apart from them, iodonium salts $[(L_2I)^+(I_n)^-]$, neutral disulfides [LS-SL], mono-cationic disulfides ($[LS\text{-}SL]^+(I_n)^-$) and dicationic disulfides ($[LS\text{-}SL]^{2+}2(I_n)^-$) with iodide or polyiodides as counter anions were also obtained [1-9]. T-shape adducts, in which two iodine atoms are connected with sulfur creating linear motive I-S-I are also reported [3]. The common ligands of these compounds contain thiocarbamide group [1-9]. One of the simplest thiocarbamides is thiourea (TU), and its derivative N-methylthiourea (MeTU).

Thioamides, like carbimazole (CBZ, 3-methyl-2-thioxo-4-imidazoline-1-carboxylate and methimazole (MMI, N-methylimidazoline-2-thione), are used as clinical drugs for the treatment of hyperthyroidism disease [2]. Moreover, iodine compounds can be applied in semiconductors or superconductors depending on the number of iodine in these materials [7-10]. Also these compounds were used as oxidation agents, oxidizing the metals, even noble ones [4h] and they were investigated for their magnetic properties [10]. Both these applications result from the ability of the elements of the Group 16 of the periodic table, like sulfur, to form charge transfer complexes [11].

During 1947 King *et.al* [12] demonstrated that ketones react with thiourea and halogens–or certain oxidizing agents to give substituted 2-aminothiazoles (Reaction 1).

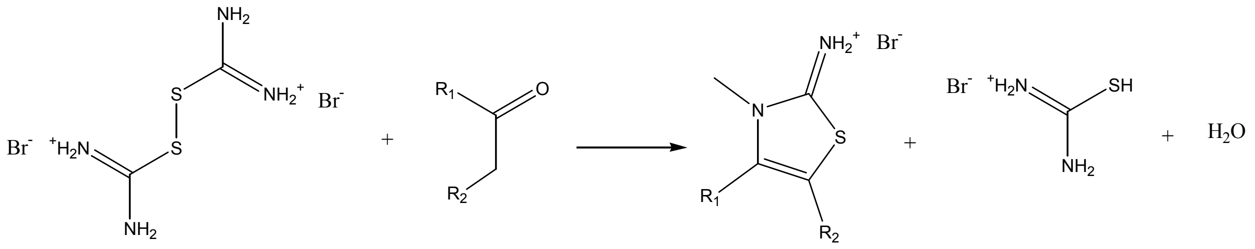

Reaction 1

Due to the importance of aminothiazoles and their derivatives in synthetic organic chemistry

Metwally *et.al* have reviewed the preparation routes for them [13]. Substituted 2-aminothiazoles and their derivatives have been used as biologically active molecules [14a], as antibacterial, antifungal [14b-14e], anthelmintic agents [14f], as inhibitors [14g] and as activators of many biological processes [14h]. 2-Aminothiazole derivatives are used in treatment of head twitches [15a], tumors [15b,15c], malaria [15d], ulcers [15e], anoxia [15f], tuberculosis [15g], anxieties [15h], chelating agents [16a-16c]. They are also used in syntheses of dyes [17a] and as chemosensors [17b-17c]. They also found application in jet fuels as anticorrosive additive [17d] and in radiochemistry as protective compounds [17e].

1,2,4-thiadiazole (Thd) and its derivatives, on the other hand, exhibit many application and therefore the synthesis of these compounds has been developed for many years [18a]. Thd and its derivatives are essentially biological active compounds. They reveal actions in antihypertensive [19a] and cardioprotective treatment [19b-19c]. They have a potential activity as G-protein coupled receptors [19d]. Thd inactivates enzymes with active cysteine residues [19e] (e.g. bacterial enzymes [19f]) and they are constituents of non-steroidal anti-inflammatory agents [19g]. The everyday antibiotic drug cefozopram [19h] is also a Thd derivative. Moreover there are indications that it possesses an effective influence on Alzheimer's disease [19i].

One of the synthetic routes developed for 1,2,4-thiadiazole derivatives involves the reaction of arylothioamides with chloride or bromide anions and acid in DMSO solution [18b] (Reaction Scheme 2).

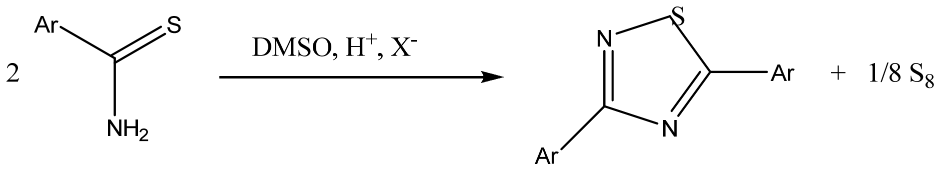

X=Cl, Br; Ar = phenyl, 3-pirydyl

Reaction Scheme 2

In this paper we report the synthesis, structural and spectroscopic characterization of the compounds **1-5** and **7** resulting from the reaction between thiourea (TU) or methylthiourea (MeTU) with di-iodine in the presence or absences of hydrochloric, hydrobromic or hydroiodic acids towards dicationic disulfides with mono- or poly- iodides as counter anions. The ionic salts **6** and **8-9** which contain substituted aminothiazole or thiadiazole rings were obtained by modifying the stoichiometry of the reaction between thiourea or methylthiourea (MeTU) and di-iodine followed by crystallization in acetone or ethanol.

Results and Discussion

Reactions: It is well known that interesting products with a variety of nuclearities could be isolated when chalcogen donors (D) were reacted with halogen independently to the molar ratios of the reactants [1-9]. For example the poly-iodide chain $[I_{17}]^-$ is formed in $\{\{(PYOH)_6\ [(PYOH)_2]^{2+}\}\ 0.5I^-\ 1.5I_7^-\ I_2\}$ when 2-pyridone reacts with di-iodine in 1:2 molar ratio [2e]. Conductivity titration experiments confirm that even poly-iodides of very high nuclearities were obtained at 1:2 (D:I2) molar ratio of the reactants [2d,c,e]. To ascertain the number of the ionic species derived by the di-iodine and TU or MeTU interaction, conductivity titrations in acetonitrile solution were carried out (Figure 1). At zero I_2 concentration, the solutions of either TU or MeTU exhibit almost zero conductivity. The conductivity of the solutions increases to a rate value when the $[I_2]$:[ligand] molar ratio is 2:1 where a stable specie is formed in the solution. Further addition of di-iodine increases the conductivity of the solution to higher values indicating that many type ionic species could also obtained in higher ratios.

Figure 1

Since the presence of hydro-halogens in the reaction mixtures might be lead to different products (see Reaction 1 and Reaction Scheme 2), we extend our studies to the redox reactions of thiourea (TU) or methylthiourea (MeTU) with di-iodine in 2:1, 1:2 and 1:1 (TU:I_2) molar ratios in the presence or absence of HX (X= Cl, Br, I). All products derived from the reactions were characterized by X-ray analysis. Crystals growth from the reaction solutions were refined, even those of the same products. Crystals of $[(TU_2)^{2+}\ 2(I^-)\cdot H_2O]$ (**1**), were grown from the crystallization of the product derived from the reaction of TU with di-iodine (Reaction Scheme **3a**). It was also directly formed in the presence of hydroiodic or hydrochloric acids in 1:1:1 ($TU:I_2:HX$ X= I, Cl) ratio (Reaction Scheme **3b** and **3c1**), since hydrohalogens enhance the oxidizing potential of the solution leading to the cationic disulfide formation. Crystals of $[2(TU_2)^{2+}\cdot(Cl^-)\cdot 2(I^-)\cdot(I_3^-)]$ (**2**) (Reaction Scheme **3c2**), $[(TU_2)^{2+}\ (Br^-)\ (I_3^-)]$ (**4**) (Reaction Scheme **3e1** or **3f**) and $[(TU_2)^{2+}\ 2(Br^-)\cdot H_2O]$ (**5**) (Reaction Scheme **3e2**) were formed accordingly. Excess of hydroiodic acid leads to the $[(TUH)^+\ (I_3^-)]$ (**3**) when TU reacts with di-iodine in 1:1:2 ($TU:I_2:HI$) ratio (Reaction Scheme **3d**). The proton excess prevents the redox reaction by stabilising the cationic specie TUH^+. When the product of the reaction between TU with an excess of di-iodine is crystallized in aceton/ethylether solution media, the ionic salt of formula $[(DAThdH^+)(I^-)]$ (**6**) (DAThd=5-diamino-1,2,4-thiadiazole) is obtained (Reaction Scheme **3g**) in a similar manner to the Reaction shown in Scheme 2 (see introduction part above) [18b]. This reaction involves oxidation of TU to a cationic disulphide which then turns to the cyclic ionic compound **6** by desulfuration.

Similarly to TU, methylthiourea (MeTU) is oxidized to $[2(MeTU_2)^{2+}\cdot 2(Br^-)\cdot(I_4^{2-})]$ (**7**) (Reaction Scheme **3h**). The ionic salt $[(DMeAThH^+)(I^-)(H_2O)]$ (**8**) (Reaction Scheme **3i, 3k**) which contains the cationic 2-amino-3,4-dimethylthiazole ($DMeAThH^+$), was growth from acetone solution when MeTU react with excess of di-iodine, while when ethanol was used the $[(AMeAThdH^+)(I_3^-)]$ (**9**) compound (Reaction Scheme **3m**) which contains the cationic 5-amino-3-methylamino-4-methyl-1,2,4-thiadiazole $(AMe2AThdH)^+$, was isolated. Compound **8**, was derived, possibly through de-oxygenation of acetone which simultaneous reacts with the MeTU residue formed from the degradation of the corresponding disulfide di-cation in a similar manner to the synthetic pathway, shown in Reaction 1 [12]. However, the isolation of compound **6** and **9** might be due to the reaction between the residues formed from the degradation of the corresponding di-cationic disulfides which have been desulfurated previously (Reaction Scheme 4). Crystals of elemental **S_8** were also isolated from the Reaction Scheme **3m**. The isolation of elemental sulfur further supports our assumption.

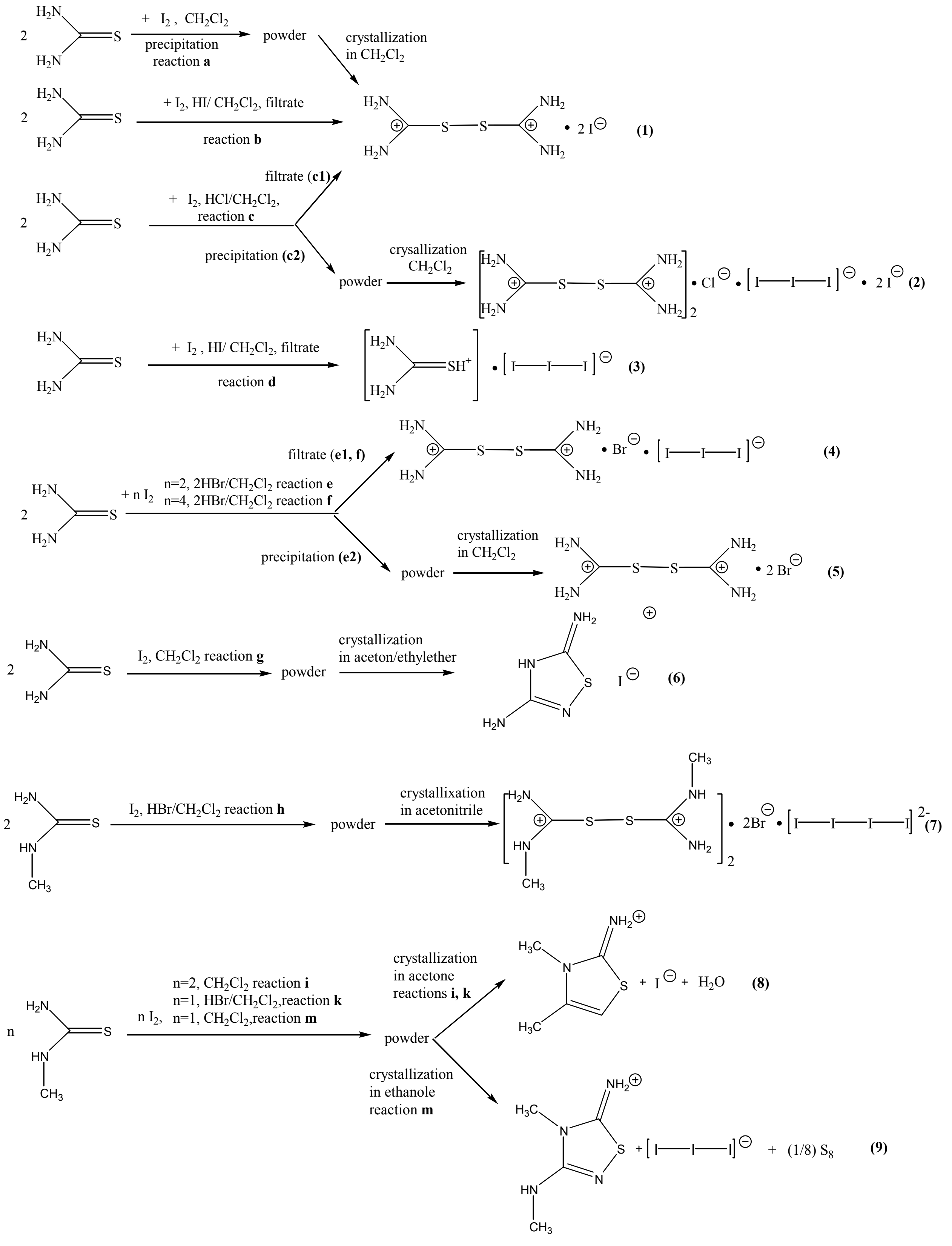

Reactions Scheme 3.

The formation of $\mathbf{S_8}$ is in accordance with the stoichiometry of the reaction and is also observed during the synthesis which involved arylothioamides in DMSO solution (Reaction Scheme 2) [18b].

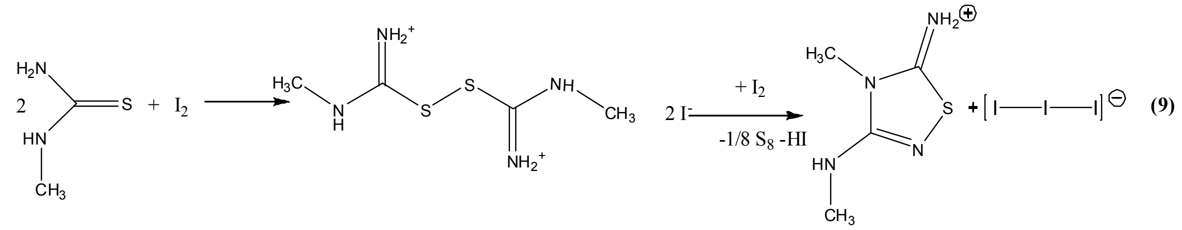

Reaction Scheme 4

Johnson and Edens [20a] reacted ethylenethiourea with di-iodine in water and they formulated the (red crystalline) product as the di-sulfide. The repetition of this reaction by Herbstein and Schwotzert [20b] showed that a condensation product was unexpectedly formed, by the N-substitution of ethylenethiourea, from its de-sulfurated species, indicating that a desulfuration of the thiol had taken place.

We have also recently shown that selenium analogues of the anti-thyroid drug 6-*n*-propyl-2-thiouracil (PTU), of formulae RSeU, [R= methyl- (Me-), ethyl- (Et-), *n*-propyl- (*n*-Pr-) and *i*-propyl- (*i*-Pr-)], reacted with diiodine in a 1:1 molar ratio in dichloromethane solutions and resulted to the formation of $[(\mathrm{RSeU})\mathrm{I}_2]$ [2g]. Crystallization in chloroform led to the formation of the CT complex $[(n\text{-PrSeU})\mathrm{I}_2]$. Re-crystallization of the $[(\mathrm{RSeU})\mathrm{I}_2]$ compounds in acetone gave the di-selenides of formulae $[N\text{-(6-Et-4-pyrimidone)(6-Et-SeU)}_2]$ and $[N\text{-(6-}n\text{-Pr-4-pyrimidone)(6-}n\text{-Pr-SeU)}_2]$. Re-crystallization in methanol/acetonitrile solutions, on the other hand, led to the deselenation with the formation of 6-*n*-propyl-2-uracil (n-Pr-U) [2g]. The formation of these products indicated that deselenation occurred upon reaction of selenoamides with di-iodine [2g].

Similar to deselenation, the desulfuration of 2-mercapto-5-nitrobenzimidazole upon reaction with di-iodine was also observed, producing 2-hydroxy-5-nitrobenzimidazole [2k]. This was the first reported example of such a reaction of a thiol in the presence of I_2 (Reaction Scheme 5).

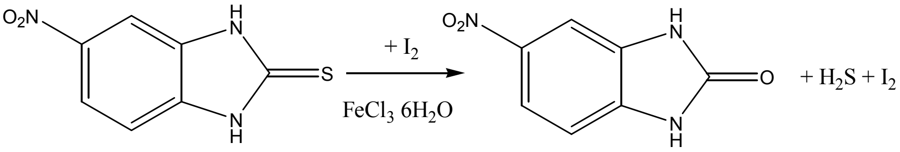

Reaction Scheme 5

Solution Studies: Solution studies (UV and ^{1}H-NMR) were employed for the interprintation of the species formed in solution, based to the solid-state compounds observed by XRD.

NMR Spectroscopy: The ^{1}H-NMR spectrum of the free ligand TU (Figure S1) shows resonance signals for the amine protons at 7.06 ppm (br, H(NH$_2$)) in DMSO-d$_6$ solution. The spectra of compound **1-5**, however are dominated by two broad resonances based on the preparation procedures applied; (**1_a**): 7.6-7.1 and 6.19 ppm, (**1_b**): 8.2-7.6 and 6.19 ppm, (**1_c1**): 8.4-7.2 and 6.19 ppm, (**2_c2**): 8.4-7.7 and 6.19 ppm, (**4_e1**): 8.8-7.8 and 6.19, (**4_f**): 9.1-8.1 and 6.19, (**5_e2**): 8.1-7.5 and 6.19 (Figure S1-S2). It is therefore concluded the existences of two types of hydrogen atoms in solution in case of **1-5** (which are varied accordingly to the preparation method). The formation of the disulfide dication $(TU)_2^{2+}$ derived by the lengthening of the C-S bond and subsequently of the S-S bond (Scheme 6). Therefore, the resonance signal 6.19 ppm is attributed to the neutral H(NH$_2$) while signal at higher values are assigned to the H$^+$(NH$_2$) group (Scheme 6). Moreover, variations in the resonance signals are also due to the hydrogen bonds established in solution with the oxygen of water molecules in case **1** and **5** or halogen anion in all cases and those which are interacting with iodides (see crystal structures).

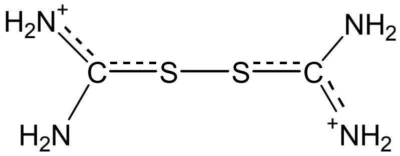

Scheme 6

The ^{1}H-NMR spectrum of [(DMeAThH$^+$)(I$^-$)(H$_2$O)] (**8**) (Figure S3) is dominated by two resonance signals at (**8_i**): 9.28 (s) and 6.69 (s) ppm and (**8_k**): 9.30 (s) and 6.70 (s) ppm which attributed to the H(NH_2^+=) and to the H(-^{5}CH-). While the ^{1}H-NMR spectrum of the cation of [(AMeAThdH$^+$)(I_3^-)] (**9**) (Figure S3) is dominated by two resonance signals at 9.72 (s) and 7.64 (q) ppm which attributed to the H(NH_2^+=) and to H(-NH^+-) respectively.

UV-Vis Spectroscopy: Figure 2A shows UV spectra of thiourea and complexes **1-6**. The UV-vis spectra of the complexes were recorded in diluted dichloromethane solution (5 10^{-5} M). Methanol (5 μL) was added in each stock solution (10^{-2} M) in order to increase the solubility of the samples in the concentrated solution (10^{-2} M). The UV spectrum of TU shows an intense band at 256 nm (ε= 3.44 mol^{-1} cm^{-1}) in CH_2Cl_2. The addition of di-iodine in dichloromethane solution of TU causes an absorbance decrease of this band and a new band at 300 nm (Figure 2A) is appeared. In case of compounds **2**, **3**, **4** and **5**, a third band or shoulder is also appears at 365 nm. The spectra of compounds MeTU, **7**, **8** and **9** are shown in Figure 2B. The addition of di-iodine in dichloromethane solution of MeTU causes the appearance of a new band at 300 nm, which is accompanied by an additional band at 365-367 nm in **7-9**.

Figure 2

The band at 255 nm is attributed to the intra-ligand transition (π*🡐π) (for both TU and MeTU). The absorption bands at 365 and 300 nm in the UV spectra of iodine compounds could be assigned to the I_3^- species (λmax= 360 and 295 nm) [2d]. Based on a large body of data on the CT bands of di-iodine complexes with cyclic thiourea derivatives, Laurence et.al have shown that their UV spectra constitute by a CT band in the 294–302 nm range typical of planar complexes or a CT band absorbs at significantly longer wavelengths (321–350 nm) characterizing perpendicular complexes [21]. Thus, among TU and MeTU complexes **1-9,** the spectra of compounds **2**, **3**, **4**, **7** and **9** show the presence of the poly-iodides anions I_n^{-x} (n=3 or 4 and x= -1 or -2 respectively) with a band at 300 nm accompanied by one band or shoulder at 365 nm. The two absorptions bands at λmax 257 and 301 nm in the spectrum of compound **1** where only iodide anions are presents as counter parts of a dicationic disulfide is attributed to the dication. This is further supported by the presence of this absorption in all spectra of **1**, **2**, **4** and **5** which are salts containing the same dication and different anions. The spectra of the ionic heterocyclic compounds **6** **8** and **9** contains absorptions at 255 and 370 nm (**6**), at 267, 299 and 367 nm (**8**) and at 299 and 365 nm (**9**) due to the delocalized double bonds of the heterocyclic cationing ring (see crystal structure). However the spectrum **5** is dominated by three absorption bands at 267, 296 and 366 nm which might be due to the stronger cation-anion interaction because of the precedence of the bromide anion instead of iodide.

Crystal and molecular structures of $[(TU_2)^{2+}\ 2(I^-)\cdot H_2O]$ *(**1**),* $[\{(TU_2)^{2+}\}_2\cdot(Cl^-)\cdot 2(I^-)\cdot(I_3^-)]$ *(**2**),* $[(TUH)^+\ (I_3^-)]$ *(**3**),* $[(TU_2)^{2+}\ (Br^-)\ (I_3^-)]$ *(**4**),* $[(TU_2)^{2+}\ 2(Br^-)\cdot H_2O]$ *(**5**),* $[(DAThdH^+)(I^-)]$ *(**6**),* $[2(MeTU_2)^{2+}\cdot(2Br^-)\cdot(I_4^{2-})]$ *(7),* $[(DMeAThH^+)(I^-)(H_2O)]$ *(**8**) and* $[(AMeAThdH^+)(I_3^-)]$ *(**9**):* ORTEP diagrams of compounds **1-9** are shown in Figures 3-11, while selected bond distances and angles for **1-9** are summarized in Tables 1-2.

Figure 3-11

Tables 1-2

Compounds **1, 2**, **4** and **5** consist of one dicationic disulfide $[(H_2N)_2CS]_2^{2+}$ and a counter anions, depending on the preparation conditions. Variations in both, the cationic disulfide and its counter parts are observed. Compound **3**, on the other hand, has a protonated TU ligand in the form of $[(H_2N)_2CSH]^+$ cation and a I_3^- counter anion.

Crystals of **1** derived either by Reaction Scheme **a, b** or **c1** are identical (Figure 3A) (small differences in the unit cell parameters in space group Pccn are caused by different data collection temperatures, and are in the range of real experimental errors: from Reaction Scheme **3a**: a= 16.3940(2), b= 5.1170(7), c= 13.3380(5) Å, R= 2.74%; from Reaction Scheme **3b**: a= 16.3810(5), b= 5.106(1), c= 13.3220(4) Å, R= 2.18 % and from Reaction Scheme **3c1**: a= 16.5130(3), b= 5.1450(1), c= 13.3880(2) Å, R= 4.02%). The crystal structure of complex **1** is similar to the one reported 50 years ago (space group Pccn with a= 5.15, b= 16.52, c= 13.39 Å and R= 8.9 % [22]). However, the structure of **1** reported here, is superior in quality (R factor 2.18% as compared to 8.9%, the former structure was based on photographic method, hydrogen atoms positions were not determined etc.), so we decided to include its analysis here as well. Also, crystals of **4** derived from Reactions Schemes **3e1** or **3f** are identical (with the same reservation as above: crystals from Reaction Scheme **3e1**: a= 9.8700(3), b= 12.0780(3), c= 12.9330(3)Å, β= 109.830(3)°, R= 4.55 %; crystals from Reaction Scheme **3f**: a= 9.8610(8), b= 11.8750(9), c= 12.812(1) Å, β= 109.250(9)°, R= 9.24 %). Finally, crystals of **8** derived from Reaction Schemes **3i** or **3k** are identical as well (crystals from Reaction Scheme **3i**: a= 7.1147(5), b= 8.5354(7), c= 8.7585(7) Å, α= 114.807(8), β= 91.836(6), γ= 99.090(6)°, R= 3.48 %; crystals from Reaction Scheme **3k**: a= 7.0530(4), b= 8.5000(5), c= 8.6960(5) Å, α=114.890(5), β=91.954(5), γ=99.007(5)°, R= 2.31 %).

The structure of compound **1** contains one symmetrical (C_2 symmetry) dicationic disulfide $[(H_2N)_2CS]_2^{2+}$, two iodide ions as counterparts and a co-crystallized water molecule (which also lies at the twofold axis, Figure 3A). Strong hydrogen bonds N11[H]···O1W= 2.950(4) Å link the disulfide species constructing parallel 1D infinite chains (Figure 3B). Between these chains the iodide anions are packed. In the case of **1** intermolecular S···S interactions of 3.481(2) Å are also established (Figure 3B). The C-S bond distance in **1** (C1-S1= 1.783(3)Å) is lengthened in regards to the free ligand (1.71(1) Å [22a]) as expected but close to the corresponding bond distance in the dicationic specie $[(H_2N)_2CS]_2^{2+}$ consisting the $\{[(NH_2)_2CSSC(NH_2)_2]Cl\ [ReCl_5\{SC(NH_2)_2\}]$ complex (1.75-1.76 Å [22b]). Thiourea moieties are planar.

The asymmetric part of the unit cell of the structure of compound **2** (Figure 4A) contains a dicationic disulfide $[(H_2N)_2CS]_2^{2+}$ and different anions: a mono-iodide, a half of a chloride and a half of tri-iodide, which occupy special positions at two different centers of inversion: chloride at (0, 0, 0) and triiodide at (0, 1/2, 0). The dicationic disulfide species lie in parallel layers with the anions packed between these layers (Figure 4B). The tri-iodide anion is symmetric, due to the special position it occupies, (I-I-I= 180º) with typical length of bonds (I-I= 2.9246(4) Å) [6]. Both simple anions (Cl^- and I^-) are involved in relatively strong (Cl) or weaker (I) N-H···X^- hydrogen bonds, while I_3^- are restrained in cavities between disulfide molecules, and do not take part in strong intermolecular interactions. It is noteworthy to mention that each chloride anion is bonded with hydrogen of four independent disulfides forming a square planar geometry around the Cl anion while I^- anion interacts with six N-H groups (Figure 4B). Chloride anions are also interacting weakly with sulfur (Cl1···S1= 3.374(2) Å, Cl1···S2= 3.423(2) Å, (S1···Cl1···S2= 77.8(1)º)) (Figure 4B). The C-S bonds in **2** (S1-C1= 1.780(6), S2-C2= 1.778(6) Å), are similar to the corresponding ones found in complex **1**. The C-N bond distances in **2** (C1-N11= 1.307(8), C1-N12= 1.303(7), C2-N21= 1.316(8), C2-N22 = 1.300(8) Å) are in accordance to those measured in **1** **(**C1-N11= 1.305(4) Å, C1-N12= 1.306(4) Å**)**.

The asymmetric part of the crystal structure of compound **4,** which was derived from Reaction Schemes **3e1** and **3f**, also contains one dicationic disulfide $[(H_2N)_2CS]_2^{2+}$ moiety and two kinds of counter mono-anions; one bromide and two halves of tri-iodides (Figure 5A). The triiodides are C_i-symmetrical, their central iodine atoms lie on the centers of symmetry at (0,0,1/2) for I1 and (1/2,1/2,1/2) for I3. The bond lengths and angles between the carbon and sulfur atoms in **4** are similar to those of complex **1**. The C-S bond distances in **4** (C1-S1= 1.759(6), S2-C2= 1.777(6) Å) are longer than in the free ligand (1.71(1) Å [24]) as expected [24]. Tri-iodides are perfectly linear, due to the symmetry (I-I-I= 180º) with typical I-I bond distances (I1-I2= 2.9172(5) and I3-I4= 2.9220(6) Å) [6]. Thiourea moieties are planar, with C1-S1-S2-C2 torsion angle 102.7(3)º. This value is closer to the corresponding one reported earlier for $[TU_2]X_2$ (X= Cl, Br, I) by Foss et.al (104.8º) [22], but larger than the one found in **1** (C1-S1-S1-C1= 94.7(2)º). The N[H]···Br hydrogen bonds (H···Br distances of *ca.* 2.6Å (Table 1)) lead to an infinity plane architecture (Figure 5B). Weaker N[H]···I1 and halogen-sulfur interactions are also established.

The asymmetric part of the unit cell of compound **5** contains a half of the dicationic disulfide $[(H_2N)_2CS]_2^{2+}$, a bromide ion and half of a water molecule (Figure 6A). The oxygen atom and the middlepoint of the S-S distance lie on a two-fold axis, so the symmetry of these two species is C_2. The structure of **5** is similar to **1**, with bromide counter anions instead of iodides. Strong hydrogen interactions among water molecules, bromide anions and N-H groups create a 3D supramolecular assembly (Figure 6B). Water molecule accepts two N-H···O hydrogen bonds and acts as a donor in two O-H···Br$^-$ hydrogen-bond interactions (Figure 11A). Amine groups also take part in four hydrogen-bond type interaction with bromide anion. Bromide lies in close contact with carbon (C1···Br1= 3.578(4) Å) and interacts with π electrons localized on N-C-N moiety (Figure 11B).

The S-S bond distances found in **1-5** lie between 2.0244(14) and 2.038(2) Å (while the C-S-S-C torsion angles vary from 86.4(3) to 102.7(5)^o. The S-S bond distances in **1-5** are shorter than those in neutral disulfides {(2-mercapto-benzoic acid)$_2$·1/2(CH$_3$CN)}, {(2-mercato-nicotinic acid)$_2$·(H$_2$O)}) and (2-mercapto-pyrimidine)$_2$ which lie in the range of 2.043–2.045 Å [2k]. However, these bond lengths are closer to the corresponding S-S distances determined in the $[(PYS{-}PYSH)^+{\cdot}I_3^-]$ (PYSH= 2-mercaptopyridine) [2d] where the mean value of the S-S bond length in the four symmetry-independent cation/anion pairs is o 2.032 Å [2d]. We have previously shown that the torsion angles are well correlated with the S-S bond lengths [2j]. Computational studies have also shown that the S-S bonds of the disulfide molecules for the lowest energy conformation were shorter when the C-S-S-C torsion angles were between 85.1 and 90^o [23]. This general trend seems to be followed also in case of the structures **1-5**. However, unconformities are observed for **5** which has the lowest torsion angle and for **2** with the longest bond length. These might be due to the strong S···O interaction (S1···O1W contact of 3.320(1) Å) in case of **5** and to the Cl···S interactions around 3.4 Å (in case of **2** (Figure 4B).

Asymmetric part of the crystal structure of **7** contains a half of a C_2-symmetrical dicationic disulfide (middlepoint of the S-S bond is on the twofold axis) of $(MeTU)_2^{2+}$, one quarter of the tetraiodide dianion – all iodine atoms lie on the mirror plane of symmetry, and the middlepoint of the central I-I bond is on the center of symmetry at (0,0,0), and a half of the bromide which lies on the mirror plane of symmetry anion (Figure 9A). Tetraiodide is very close to linearity (I2-I1-I1= 178.46(4)Å). Disulfides are built of two methylthiourea moieties, which are planar (max deviation from the least-squares plane is 0.081(6)Å). The S1-S1 bond length (2.011(4) Å) is similar to the one in **1** (2.022(2)Å), but the S-C-C-S torsion angle (98.0(5)º) is slightly larger than the appropriate value in **1** (94.7(2)º). This might be due to the presence of additional methyl group. Hydrogen bonding interactions of N-H···Br and N-H···I type stabilize the crystal structure (Figure 9B).

The structure of compound **3** consists of a protonated thiourea TU $[(H_2N)_2CSH]^+$ and tri-iodide counter anion $[I_3^-]$ (Figure 5A). The bond lengths and angles are generally in accordance with those reported for the free ligand [24], but the C-S bond, of 1.739(3) Å, is longer than that of free ligand (1.71(1) Å [24]) due to the protonation of the sulfur atom. The C-N bonds are almost equal, and shorter than the corresponding bonds in free ligand (1.33(1) Å [24]). The tri-iodide anion is highly asymmetrical and strictly linear (I1-I2= 2.8558(3) Å, I2-I3= 2.9961(3) Å, I1-I2-I3= 179.102(9)º).. In the crystal, a number of hydrogen bonds accepted by the terminal iodine atoms are observed (Figure 5B).

Crystals of **6** contains the protonated 3,5-diamino-1,2,4-thiadiazole cation $(DAThd)^+$ and an iodide counter anion (Figure 6A). The same product was also obtained by reacting (1-diaminomethylene)thiourea with either copper(II) chloride or chromium trichloride [25a]. Comparative study of C-N bonds in the neutral ligand (1.367(2), 1.377(2)Å, 1.339(2) Å respectively [25b]) are significantly longer than in **6** (1.334(3), 1.328(3), 1.327(3) Å). All atoms of $(DAThd)^+$ have insignificant deviations from plane (max deviation of 0.015(2) Å). Strong hydrogen bonds N31···N4 (*1-x,1-y,2-z*) link two $(DAThd)^+$ ions into centrosymmetrical pairs, while other, weaker interactions: N-H···I hydrogen bonds, S···S contacts (3.423(1)Å) create the three-dimensional structure of cations and anions.

Crystals of **8** contain 3,4-dimethyl-2-aminothiazole $(DMeAThH)^+$ cation, an iodine anion and a water molecule (Figure 10A). The neutral 3,4-dimethyl-2-aminothiazole (DMeATh) was obtained previously by treatment benzothiazol-2-ylamine of F_3CSO_3Me and KH, and its crystal structure was reported [26]. Significant differences are observed between the protonated ($DMeAThH^+$) and the neutral species: the two C-N bonds (C2-N21= 1.323(4), N3-C31= 1.469(4) Å) in **8** are longer than the corresponding ones found in DMeATh (1.280(3), 1.455(3) Å) [26], while the third C-N bond and the C-S bonds in **8** (C2-N3= 1.341(4), S1-C2= (1.731(3) Å), are shorter than the corresponding ones in DMeATh (1.372(4), 1.781(3) Å) [26]. This indicates that the positive charge is located on $[S\text{-}C(NH_2)\text{=}N]^+$ moiety (Scheme 7). However, the cation is essentially planar (max. deviation of 0.063(5) Å), which may suggest that in fact the charge is delocalized over the whole molecule.

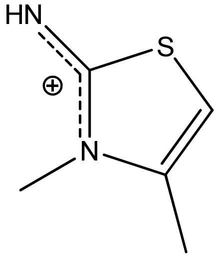

Scheme 7.

Strong N···I, O···N and O···I interactions join the 2D layers of cations with water molecules and iodide anions, which fill the space between these layers is (Figure 10B).

The crystal structure of **9** contains protonated 5-amino-3-methylamino-4-methyl-1,2,4-thiadiazole $[(AMeAThdH)^+]$ and tri-iodide anion (Figure 11A). The anion is linear (I1-I2-I3= 176.70(2)°) and highly asymmetrical (I1-I2= 2.9718(6) Å, I2-I3= 2.8710(6) Å). Two equal C-N bonds (1.335(8), 1.336(8) Å) and one longer 1.398(8) Å are found in thiadiazole ring. The positive charge is located on imidamide group of N2-C3-N31 and N4-C5-N51 (Scheme 8), where the shortest bonds are observed Thiadiazole moiety are planar (max. deviation of 0.032(6)Å). The N2-S1-C5 angle (93.0(3)°) in **9** is larger to the corresponding one of **5** (C2-S1-C5= 90.0(2)°).

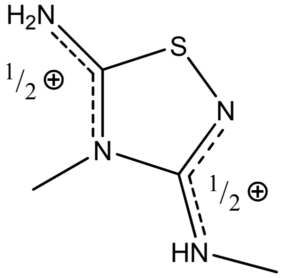

Scheme 8

Strong hydrogen bond N51[H]···N3= 2.96(1) Å create infinite chains of cations (Figure 11B)., and between the chains there are anions, interacting with the cations by means of weak hydrogen bond and S···I interactions (Figure 11B).

The elemental S_8 crystals which happened to result from one of the reactions turned out to be those of *α-sulfur* polymorphic form (Fddd space group, a= 10.319(1), b= 12.669(1), c= 24.321(2) Å)

Conclusions

A variety of products were obtained from the reaction of di-iodine with thiourea or methylthiourea. Reaction of TU or MeTU with di-iodine in the absence or presence of hydroiodic, hydrobromic or hydrochloric acids in 1:1, 1:1:1 or 1:1:2 yields ionic salts which contains dicationic disulfides (compounds **1, 2, 4, 5, 7**), while the type of the counter anions and the whole crystal structure of these compounds is depended on the reaction conditions (stoichiometry, presence or absence of acid etc). The anionic species in the crystal structures of compounds **1**, **2**, **4**, **5** contains iodide, tri-iodide and/or chloride and/or bromide. In case of compound **7** the counter anion consists by the di-anionic tetra-iodide I_4^{2-}. By increasing the acidity however, of the media the formation of the di-cationic disulfide is prevented and the mono-cationic TUH^+ specie precipitates (**3**). Cyclic compounds **6**, **8** and **9** were also derived by the reaction of TU or MeTU with diiodine followed by crystallization in polar solvent media: Thus the use of acetone lead to the formation of the compound **8** which contains the 2-amino-3,4-dimethylthiazole cation from the interaction of the

MeTU with the de-oxygenated solvent while by using ethanol instead, the compounds **6** and **9** are obtained which contains the 5-amino-3-methylamino-4-methyl-1,2,4-thiadiazole cation from the interaction of TU or MeTU with desulfurated reagents.

King et.al [12], demonstrate that ketones react with thiourea and halogens, or certain oxidizing agents to give substituted 2-aminothiazoles through dicationic disulfide intermediate (Reaction 1). Since dicationic disulfides were isolated when TU or MeTU react with di-iodine (Reaction Schemes **a-c**, **e-f**) a similar mechanism could be assumed for the preparation of **8**. Florani et.al were also reported the formation of 1,2,4-thiadiazole derivatives from the reaction of arylothioamides and chloride or bromide anions and acid in DMSO (Reaction Scheme 2) [18b]. This further supports our assumption for the formation of **6** and **9** through a dicationic disulfide intermediate followed by the formation of reactive radicals.

We have previously shown that a relationship between S-S distance and torsion C-S-S-C exist [2j] which also supported by the reported computational studies on small molecules [23]. Experimental data (Figure 12) are shown that a hyperbola correlation is taken by comparing d(S-S) vs <(C-S-S-C). The closer S-S distance, is adopted for the best molecule conformation (minimum energy state) which in case of $[(H_2N)_2CS]_2^{2+}$ corresponds to the torsion angle C-S-S-C of 94.05º, and for S-S bond length of 2.0215 Å. The exceptions observed in **2_c2** is attributed to the strong intermolecular interactions S···Cl which are lengthening the S-S bond distance, while in **3_e** to the low refinement (big R factor) of 9.24%.

Figure 12

Experimental

Materials and instruments: All solvents used were reagent grade. Di-iodine (Aldrich), hydroiodic acid (57%) (Aldrich), hydrobromic acid (48 %) (Fluka), hydrochloric acid (38%) (Merck), thiourea methylthiourea (Merck) were used with no further purification. Melting points were measured in open tubes with a Stuart scientific apparatus and are uncorrected. Infra-red spectra in the region of 4000-400 cm^{-1} were obtained from KBr with a Perkin - Elmer Spectrum GX FT-IR spectrophotometer. The ^1H NMR spectra were recorded with a Bruker AC250 MHFT NMR instrument in DMSO-d_6 solutions. Mass Spectra (MHRMS) were recorded in MeOH/CH_2Cl_2 solutions 200 μL/800 μL on LTQ-ORBITRAP-XL (Thermoscientific USA) with resolution 10000 .

Synthesis and crystallization of $[(TU_2)^{2+}\ 2(I^-)\cdot H_2O]$ (**1**), $[2(TU_2)^{2+}\ 2(I^-)\ (I_3^-)\cdot(Cl^-)]$ (**2**), $[TUH^+\cdot I_3^-]$ (**3**), $[(TU_2)^{2+}\ (I_3^-)\cdot(Br^-)]$ (**4**), $[(TU_2)^{2+}\ 2(Br^-)\cdot H_2O]$ (**5**), $[(DAThdH^+)\cdot(I^-)\cdot H_2O]$ (**6**) $[2(MeTU_2)^{2+}\ (I_4^-)\ 2(Br^-)]$ (**7**), $[(DMeAThH^+)(I^-)(H_2O)]$ (**8**), $[(AMeAThdH^+)(I_3^-)]$ (**9**):

Compound **1** was prepared by mixing dichloromethane solutions of di-iodine and TU in 1:1 molar ratio (Reaction Scheme **3a)** or di-iodine, TU with hydriodic acid 1:1:1 ratio (Reaction Scheme **b)** or di-iodine, TU with hydrochloric acid (Reaction Scheme **3c1**) in 1:1:1 molar ratio under aerobic conditions at 0ºC with continuous stirring for 2-3 h. The solution was then filtered and the resulting powder (**a**, **b**, **c1**) and dark crystals (**b**, **c1**) suitable for single-crystal analysis by X-ray crystallography of the complex **1** are obtained. Powder from Reaction Scheme **3a** was crystallized and also dark crystals suitable for single-crystal analysis by X-ray crystallography of complex **1** was obtained.

1: (**a**) yield 87% corresponding to 22 mg of product; m.p. 77-80ºC. Elemental analysis found: C: 5,72; H: 2,86; N: 13.81; S: 15,21 %; calculated for $C_2H_{10}I_2N_4OS_2$: C: 5.67; H: 2.37; N: 13.21; S: 15.12 %. MID-IR (KBr) (cm^{-1}): 3372.44 vs, 3306.99 vs, 3162.28 vs, 3083.46 vs, 1643.41 vs, 1615.15 vs, 1527.38 sh, 1409.22 s, 1029.92w, 734.71w, 698.99 m, 599.77 m, 552.77w, 521.86 w, 459.75 m (Figure S4). UV/Vis (CH_2Cl_2): λmax (logε) = 257 nm (2.52), 300 nm (2.91). ^1H-NMR (DMSO-d_6) (δ ppm): 6.186 [s, 1.0], 7.1-7.6 [br, 1.0] (Figure S1). MS m/z: 151.01 $[(NH_2)_2C\text{-}S\text{-}S\text{-}C(NH_2)(=NH)]^+$ (Figure S12) (**b**) yield 91% corresponding to 48 mg of product; MID-IR (KBr) (cm^{-1}): 3318.17 vs, 3268.85 vs, 3090.44 vs 3043.21 vs, 1656.11 vs, 1403.69m, 1073.03 w, 697.47 w, 602.08 m 466.99 w (Figure S4). UV/Vis (CH_2Cl_2): λmax (logε) =(3.14), 300 nm (3.39). ^{1}H-NMR (DMSO-d$_6$) (δ ppm): 6.194 [s, 1.0], 7.6-8.2 [br, 4.0] (Figure S1).

(**c1**) yield 81% corresponding to 43 mg of product;. MID-IR (KBr) (cm^{-1}): 3270.29 vs, 3091.48 s, 1656.96 vs, 1403.06 s, 1068.73 w, 701.47 w, 666.71 w, 602.72 m, 464.86 w (Figure S4). UV/Vis (CH_2Cl_2): λmax (logε) =255 nm (3.23), 300 nm (3.50). ^{1}H-NMR (DMSO-d$_6$) (δ ppm): 6.185 [s, 1.1], 7.2-8.4 [br, 1.0] (Figure S1).

Compound **2** was prepared by crystallization in dichloromethane of the powder precipitates initially from Reaction Scheme **3c1**. Dark crystals of the complexes suitable for single-crystal analysis by X-ray crystallography were then grown and filtered off.

2: (**c2**) yield 68% corresponding to 19 mg of product; m.p. 70-75°C. Elemental analysis found: C: 5.12; H: 1.73; N: 11.41; S: 13.34 %; calculated for $C_4H_{16}ClI_5N_8S_4$: C: 4.93; H: 1.65; N: 11.50; S: 13.16 %. MID-IR (KBr) (cm^{-1}): 3311.44 vs, 3256.71 vs, 3089.54 s, 2994.70 s, 1658.78 vs, 1403.77 m, 1191.98 w, 1080.00 m, 715.25 w, 666.23 w, 610.20 m, 462.79 w, 412.04 w (Figure S5). UV/Vis (CH_2Cl_2): λmax (logε) = 257 nm (2.69), 301 nm (2.95). ^{1}H-NMR (DMSO-d$_6$) (δ ppm): 6.189 [s, 1.0], 7.7-8.4 [s, 4.7] (Figure S2). MS m/z: 170.97 $\{[(NH_2)_2C\text{-}S\text{-}S\text{-}C(NH_2)_2]\ H_2O\}^+$ (Figure S13).

Compound **3** was prepared by mixing dichloromethane solutions of di-iodine with TU with hydrobiodic acid in 1:1:2 (Reaction Scheme **3d**) molar ratio under aerobic conditions at 0 °C with continuous stirring for 2-3 h. The solution was then filtered and dark crystals suitable for single-crystal analysis by X-ray crystallography of the complex **3** are obtained.

3: (**d**) yield 30% corresponding to 68 mg of product; m.p. 54-55 °C. Elemental analysis found: C: 2.76; H: 1.29; N: 6.21; S: 6.78 %; calculated for $CH_5I_3N_2S$: C: 2.62; H: 1.10; N: 6.12; S: 7.00 %. MID-IR (KBr) (cm^{-1}): 3311 vs, 3256.71 vs, 1658.78 vs, 1403.77 s, 1191.98 w, 1080.00 m, (Figure S6). UV/Vis (CH_2Cl_2): λmax (logε) = 257 nm (2.59), 300 nm (2.95). MS m/z: 115.03 $[(NH_2)_2C{=}SH]^+$ (Figure S14).

Compound **4** was prepared by mixing dichloromethane solutions of di-iodine with TU with hydrobromic acid in 1:1:1 (Reaction Scheme **3e1)** or 2:1:1 (Reaction Scheme 3**f**) under aerobic conditions at 0ºC with continuous stirring for 2-3 h. The solution was then filtered and the resulting powder (**e1**) and dark crystals (**e1**, **f**) suitable for single-crystal analysis by X-ray crystallography of the complex **4** are obtained.

4: (**e1**) yield 81% corresponding to 87 mg of product; m.p. 32-35 ºC. Elemental analysis found: C: 3.84; H: 1.45; N: 9.55; S: 10.20 %; calculated for $C_2H_8BrI_3N_4S_2$: C: 3.92; H: 1.31; N: 9.14; S: 10.46 %. MID-IR (KBr) (cm^{-1}): 3329.00 vs, 3080.72 s, 1653.97 vs, 1403.60 m, 1097.44 w, 1049.64 w, 704.67 w, 665.93 w, 602.79 m, 551.06 w, 464.52 w (Figure S7). UV/Vis (CH_2Cl_2): λmax (logε) = 255 nm (2.55), 300 nm (2.94). ^{1}H-NMR (DMSO-d_6) (δ ppm): 6.192 [s, 1.0], 7.8-8.8 [br, 7.8] (Figure S2). MS m/z: 170.97 $\{[(NH_2)_2C\text{-}S\text{-}S\text{-}C(NH_2)_2]\ H_2O\}^+$ (Figure S15).

(**f**) yield 83% corresponding to 43 mg of product; MID-IR (KBr) (cm^{-1}): 3343.82 vs, 3279.12 vs, 1656.99 m, 1403.59 m, 1098.99 w, 1050.37 w, 710.30 w, 608.40 w, 466.29 w (Figure S7). UV/Vis (CH_2Cl_2): λmax (logε) =257 nm (2.61), 300 nm (2.91). ^{1}H-NMR (DMSO-d_6) (δ ppm): 6.194 [s, 1.0], 8.1-9.1 [br, 8.3] (Figure S2).

Compound **5** was prepared by crystallization in dichloromethane of the powder precipitates initially from Reaction Scheme **3e2**. Dark crystals of the complexes suitable for single-crystal analysis by X-ray crystallography were then grown and filtered off.

5: (**e2**) yield 49% corresponding to 18 mg of product; m.p. 107-114 ºC. Elemental analysis found: C: 7.69; H: 3.19; N: 17.14; S: 19.65 %; calculated for $C_2H_{10}Br_2N_4OS_2$: C: 7.28; H: 3.05; N: 16.98; S: 19.43%. MID-IR (KBr) (cm^{-1}): 3326.84 s, 3257.30 vs, 2995.56 s, 1658.62 vs, 1403.05 s, 1098.47 w, 1050,49 m, 711.27 m, 605.88 m, 465.97 m ,413.21 w (Figure S8). UV/Vis (CH_2Cl_2): λmax (logε) = 257 nm (1.69), 298 nm (2.10), 365 nm (1.70). ^{1}H-NMR (DMSO-d_6) (δ ppm): 6.184 [s, 1.0], 7.5-8.1 [br, 1.3] (Figure S2). MS m/z: 151.01 $[(NH_2)_2C\text{-}S\text{-}S\text{-}C(NH_2)(=NH)]^+$ (Figure S16).

Compound **6** was prepared by mixing dichloromethane solutions of di-iodine and TU in 1:2 molar ratio (Reaction Scheme **3g**). The solution was than filtered and the resulting brown powder was obtained. The powder was dissolved in ethanol afterwards and orange crystals of the compound **6** were then grown suitable for single-crystal analysis by X-ray crystallography.

6: (**g**) yield 46% corresponding 13 mg of product; m.p. 126-128 ºC. Elemental analysis found: C: 9.43; H: 2.16; N: 23.14; S: 13.01 %; calculated for $C_2H_5IN_4S$: C: 9.84; H: 2.06; N: 22.96; S: 13.14%. MID-IR (KBr) (cm^{-1}): 3320.24 s, 3230.71 s, 3176.51 s, 3105.52 m, 2975.46 m, 2917.35 m, 2855.77 m, 1621.22 vs, 1423.49 m, 1073.30 w, 968.45 w, 749.99 m, 721.66 w, 594.38 m, 527.64 m, 502.34 w, 408.56 w (Figure S9). UV/Vis (CH_2Cl_2): λmax (logε) =260 nm (3.03), 362 nm (1.78).

Compound **7** was prepared by mixing dichloromethane solutions of di-iodine and TU with hydrobromic acid in 1:1:1 molar ratio (Reaction Scheme **3h**). The solution was than filtered and the resulting brown powder was obtained. The powder was dissolved in acetonitrile afterwards and red crystals of the compound **7** were then grown suitable for single-crystal analysis by X-ray crystallography.

7: (**h**) yield 79% corresponding 17 mg of product; m.p. 138-140 ºC. Elemental analysis found: C: 9.93; H: 2.27; N: 10.72; S: 12.55 %; calculated for $C_4H_{12}BrI_2N_4S_2$,: C: 9.35; H: 2.35; N: 10.90; S: 12.48%. MID-IR (KBr) (cm^{-1}): 3157.82 s, 3082.58 s, 2995.07 vs, 1661.64 vs 1626.53 sh, 1486.42 w, 1448.41 w, 1413.71 w 1308.80 w 1164.63 w, 1111.21 w, 758.82 w, 412.24 w (Figure S10). UV/Vis (CH_2Cl_2): λmax (logε) =297 nm (2.97), 366 nm (2.71).

Compound **8** was prepared by mixing dichloromethane solutions of di-iodine and MeTU in 1:2 molar ratio (Reaction Scheme **3i**) or MeTU with hydrobromic acid with 1:1:1 molar ratio (Reaction Scheme **3k**). The solution was then filtered and the resulting brown powder was obtained. The powder was dissolved in acetone afterwards and bright yellow crystals of the compound **8** were then grown suitable for single-crystal analysis by X-ray crystallography.

8: (**i**) yield 71% corresponding to 22 mg of product; m.p. 74-81ºC. Elemental analysis found: C: 22.19; H: 3.90; N: 10.29; S: 11.83 %; calculated for $C_5H_{11}IN_2OS$: C: 21.91; H: 4.04; N: 10.22; S: 11.70%. MID-IR (KBr) (cm^{-1}): 3470.30 vs, 3405.04 vs, 3079.95, 2011.37 w, 1647.15 vs, 1560.76 vs, 1429.22 m, 1402.09 w, 1295.66 m, 1177.88 m, 1153.32 m, 1126.36 w, 973.57 w, 834.64 m, 771.43 m, 716.06 w, 600.33 m, 514.40 m (Figure S9). UV/Vis (CH_2Cl_2): λmax (logε) =254 nm (3.07), 293 nm (2.08). ^{1}H-NMR (DMSO-d_6) (δ ppm): 2.226 [s, 3.3], 3.459 [s, 2.9], 6.694 [s, 1.0], 9.282 [s, 1.9] (Figure S3). MS m/z: 129.05 $[C_5H_9N_2S]^+$ (Figure S17).

(**k**) yield 67% corresponding to 20 mg of product; MID-IR (KBr) (cm^{-1}): 3456.88 vs, 3209.17 s, 3083.26 s, 2021.25 w, 1650.08 s, 1605.21 m, 1561.87 s, 1428.63 m, 1398.46 m, 1178.36 m, 1127.19 w, 834.25 m, 773.86 m, 718.28 m, 667.35 m, 606.42 m, 518.19 m (Figure S9). UV/Vis (CH_2Cl_2): λmax (logε)= 297 nm (3.15), 366 nm (2.89). ^{1}H-NMR (DMSO-d_6) (δ ppm): 2.229 [s, 3.2], 3.464 [s, 2.9], 6.698 [s, 1.0], 9.299 [s. 1.9] (Figure S3).

Compound **9** was prepared by mixing dichloromethane solutions of di-iodine and MeTU in 1:1 molar ratio (Reaction Scheme **3m**). The solution was then filtered and the resulting brown powder was obtained. The powder was dissolved in ethanol afterwards and red crystals of the compound **9** suitable for single-crystal analysis by X-ray crystallography were grown among with crystals of **S_8** as well.

9: (**m**) yield 94% corresponding to 28 mg of product; m.p. 154-158 ºC. Elemental analysis found: C: 23.51; H: 3.67; N: 10.91; S: 12.27 %; calculated for $C_5H_9IN_2S$: C: 23.45; H: 3.54; N: 10.94; S: 12.52%. MID-IR (KBr) (cm^{-1}): 3295.96 m, 3075.21 m, 1620.63 vs, 1522.51 m, 1410.62 m, 1383.62 w, 1225.88 w, 1151.58 w, 1000.05 w, 889.23 m, 696.16 m, 588.46 w, 522.65 m (Figure S11). UV/Vis (CH_2Cl_2): λmax (logε)= 297 nm (2.25), 365 nm (1.93). ^{1}H-NMR (DMSO-d_6) (δ ppm): 2.821 [d, 3.5], 3.413 [s, 3.3], 7.637 [q, 1.0], 9.726 [s, 2.1] (Figure S3). MS m/z: 145.05 $[C_4H_9N_4S]^+$ (Figure S18).

Crystal data: Data for compounds studied were collected by the ω scan technique: for **1a**, **1b**, **1c1**, **2c2**, **4e1**, **4f**, **5e2** and **8i** on an Supernova diffractometer with Atlas CCD detector using graphite-filtered CuK$_{\alpha.}$ (λ = 1.5418Å) radiation and for **3d**, **6g**, **7h**, **8k**, **9m**, and**S_8** on an XCALIBUR diffractometer with EOS CCD detector using graphite-filtered MoK$_{\alpha.}$ (λ = 0.71073Å) radiation.

Cell parameters for **1-9** were determined by least-squares fit. All data were corrected for

Lorentz-polarization effects and absorption [28a]. The structures were solved with direct methods with SIR92 [28b] and refined by full-matrix least-squares procedures on F^2 with SHELXL97 [28c]. All non-hydrogen atoms were refined anisotropically, hydrogen atoms were located at calculated positions and refined as a 'riding model' with isotropic thermal parameters fixed at 1.2 times the Ueq's of appropriate carrier atom. The structure of **2** has been refined as twinned (using HKLF 5 command), the data were reduced as twinned. BASF factor refined at 0.78.

1: (**a**) formula $C_2H_{10}I_2N_4OS_2$, MW=424.06, orthorhombic, space group Pccn, a=16.3810(5), b=5.106(1), c=13.3220(4)Å, V=1114.27(5)Å^3, Z=4, T=120(1)K, ρ(calc)=2.53g cm^{-3}, μ=47.57mm^{-1}, F(000)=784. 2598 reflections measured up to 2θ=75.5°, of which 1128 symmetry independent (Rint=1.80%) and 1068 with I > 2σ(I). The refinement converged to final R=2.18% [I > 2σ(I)], wR2 = 5.90% (all reflections), S=1.064. Max/min Δρ in the final ΔF map: 0.79/-1.08e°Å^{-3}.

(**b**) formula $C_2H_{10}I_2N_4OS_2$, MW=424.06, orthorombic, space group Pccn, a=16.3810(5), b=5.106(1), c=13.3220(4)Å, α=90, β=90, γ=90º, V=1114.27(5)Å3, Z=4, T=130.0(1)K, ρ(calc)=2.476g cm^{-3}, μ=47.573mm^{-1}, F(000)=784. The refinement converged to final R=2.18% [for 1137 reflections with I > 2σ(I)] =, wR = 5.90% (all 1178 reflections).

(**c1**) formula $C_2H_{10}I_2N_4OS_2$, MW=424.06, orthorombic, space group Pccn, a=16.5130(3), b=5.1450(1), c=13.3880(2)Å, α=90, β=90, γ=90º, V=1137.44(3)Å3, Z=4, T=293(2)K, ρ(calc)=2.476g cm^{-3}, μ=46.604mm^{-1}, F(000)=784. The refinement converged to final R=4.02% [for 1068 reflections with I > 2σ(I)] =, wR =10.11% (all 1128 reflections).

2: (**c2**) formula $C_4H_{16}ClI_5N_8S_4$, MW=974.44, monoclinic, space group P2(1)/n, a=9.6516(3), b=9.7546(2), c=13.8230(5), β=109.653(4)º, V=1225.59(6) Å^3, Z=2, T=130(1)K, ρ(calc)=2.64g cm^{-3}, μ=54.08mm^{-1}, F(000)=884. 8852 reflections measured up to 2θ=75.5°, of which 2538 symmetry independent (Rint=3.52%) and 2400 with I > 2σ(I). The refinement converged to final R=4.44% [I > 2σ(I)], wR2 = 13.78% (all reflections), S=1.099. Max/min Δρ in the final ΔF map: 2.74/-1.40e°Å^{-3}.

3: (**d**) formula $CH_5I_3N_2S$, MW=457.83, monoclinic, space group $P2_1/c$, a= 7.5529(2), b=

13.2275(4), c= 9.1452(2), β= 98.689(2)°, V= 903.17(4) Å3, Z=4, T=295(2)K, ρ(calc)=3.37 cm^{-3}, μ= $10.53mm^{-1}$, F(000)=800. 10478 reflections measured up to 2θ=28.3°, of which 2060 symmetry independent (Rint=2.22%) and 1931 with I > 2σ(I). The refinement converged to final R=1.67% [I > 2σ(I)], wR2 = 3.83% (all reflections), S=1.180. Max/min Δρ in the final ΔF map: 0.72/-0.78e°$Å^{-3}$.

4: (**e1**) formula $C_2H_8BrI_3N_4S_2$, MW=612.85, monoclinic, space group P21/c, a=9.8698(2), b=12.0775(3), c=12.9332(3) Å, β=109.830(3), V=1450.25(6) Å3, Z=4, T=293(2)K, ρ(calc)= 2.807 g cm^{-3}, μ=56.46 mm^{-1}, F(000)= 1096. 13296 reflections measured up to 2θ=75.5°, of which 2968 symmetry independent (Rint=5.43%) and 2800 with I > 2σ(I). The refinement converged to final R=4.27% [I > 2σ(I)], wR2 = 11.79% (all reflections), S=1.050. Max/min Δρ in the final ΔF map: 1.77/-1.67e°$Å^{-3}$.

(**f**) formula $C_2H_8BrI_3N_4S_2$, MW=612.85, monoclinic, space group P21/c, a=9.8610(8), b=11.8750(9), c=12.812(1) Å, β=109.250(9)°, V=1416.4(2) Å3, Z=4, T=130K, ρ(calc)= 2.874 g cm^{-3}, μ=$57.815mm^{-1}$, F(000)= 1096. The refinement converged to final R= 9.24% [for 2303 reflections with I > 2σ(I)] =, wR = 24.73% (all 2795 reflections).

5: (**e2**) formula $C_2H_{10}Br_2N_4OS_2$, MW=330.08, monoclinic, space group P2/c, a=8.6389(11), b=5.0436(6), c=12.3817(16) Å, β=99.551(12)°, V= 532.01(12) Å3, Z=2, T=130(1)K, ρ(calc)=2.061 g cm^{-3}, μ=$13.05mm^{-1}$, F(000)=320. 3184 reflections measured up to 2θ=75.75°, of which 1098 symmetry independent (Rint=2.70%) and 1047 with I > 2σ(I). The refinement converged to final R=3.96% [I > 2σ(I)], wR2 = 12.21% (all reflections), S=1.185. Max/min Δρ in the final ΔF map: 0.82/-1.12e°$Å^{-3}$.

6: (**g**) formula $C_2H_5IN_4S$, MW=244.06, monoclinic, space group P-1, a= 4.5455(2), b= 8.6436(3), c= 9.5497(3) Å, α= 113.700(3), β= 94.020(3), γ= 103.347(3)°, V= 328.64(2) Å3, Z=2, T=100(1)K, ρ(calc)= 2.466 g cm^{-3}, μ= $5.09mm^{-1}$, F(000)= 228. 4992 reflections measured up to 2θ=28.0°, of which 1433 symmetry independent (Rint=1.99%) and 1362 with I > 2σ(I). The refinement converged to final R=1.73% [I > 2σ(I)], wR2 = 4.19% (all reflections), S=1.073. Max/min Δρ in the final ΔF map: 1.15/-0.51e°Å^{-3}.

7: (**h**) formula $C_4H_{12}BrI_2N_4S_2$, MW= 514.01, orthorhombic, space group Cmca, a= 11.3150(13), b= 11.134(2), c= 21.9321(15) Å, V= 2763.0(7) Å3, Z=8, T=295(2)K, ρ(calc)= 2.471 g cm^{-3}, μ= 7.72mm^{-1}, F(000)= 1896. 8716 reflections measured up to 2θ=29.2°, of which 1799 symmetry independent (Rint=4.95%) and 1345 with I > 2σ(I). The refinement converged to final R=4.88% [I > 2σ(I)], wR2 = 13.11% (all reflections), S=1.087. Max/min Δρ in the final ΔF map: 1.96/-1.07e°Å^{-3}.

8: (**i**) formula $C_5H_{11}IN_2OS$, MW= 274.12, triclinic, space group P-1, a=7.0530(4), b=8.5003(5), c=8.6957(5) Å, α=114.890(5), β=91.954(5), γ=99.007(5) °, V=464.16(5) Å3, Z=2 , T=100(1)K, ρ(calc)=1.961g cm^{-3}, μ= 3.62mm^{-1}, F(000)=264. 3173 reflections measured up to 2θ=28.0°, of which 1893 symmetry independent (Rint=1.94%) and 1814 with I > 2σ(I). The refinement converged to final R=2.29% [I > 2σ(I)], wR2 = 6.10% (all reflections), S=1.081. Max/min Δρ in the final ΔF map: 0.77/-0.55e°Å^{-3}..

(**k**) formula $C_5H_{11}IN_2OS$, MW=274.12, triclinic, space group P-1, a=7.0530(4), b=8.5000(5), c=8.6960(5) Å, α=114.890(5), β=91.954(5), γ=99.007(5) °, V=464.16(5) Å3, Z=2 , T=100.0(1)K, ρ(calc)=1.961g cm^{-3}, μ= 3.619mm^{-1}, F(000)=264. The refinement converged to final R=2.31% [for 1814 reflections with I > 2σ(I)] =, wR =6.22% (all 1893 reflections).

9: (**m**) formula $C_5H_9IN_2S$, MW= 256.10, orthorombic, space group Pbca, a= 12.6402(4), b= 13.7770(8), c= 14.1348(5) Å, V= 2461.49(18) Å3, Z=8 , T=100(1)K, ρ(calc)= 2.838g cm^{-3}, μ= 7.75mm^{-1}, F(000)= 1888. 6414 reflections measured up to 2θ=28.1°, of which 2547 symmetry independent (Rint=4.27%) and 1990 with I > 2σ(I). The refinement converged to final R=3.67% [I > 2σ(I)], wR2 = 7.16% (all reflections), S=1.040. Max/min Δρ in the final ΔF map: 1.38/-0.96e°Å^{-3}.

S_8: (m) formula S_8, MW= 256.48, orthorombic, space group Fddd, a a= 10.319(1), b= 12.669(1), c= 24.321(2) Å, α=90.0, β=90.0, γ=90.0 °, V= 3179.4(5) Å3, Z=16 , T=100.0(1)K, ρ(calc)= 2.143g cm^{-3}, μ= 2.142mm^{-1}, F(000)= 2048. The refinement converged to final R=3.13% [for 900 reflections with I > 2σ(I)] =, wR =8.44% (all 779 reflections).

Crystallographic data (excluding structure factors) for the structural analysis have been deposited with the Cambridge Crystallographic Data Centre, Nos. 924828 (**1**)**,** 924829 (**2**) 939693 (**3**), 924830 (**4**), 924831 (**5**), 939694 (**6**), 939695 (**7**), 924832 (**8**), and 924833 (**9**). Copies of this information may be obtained free of charge from: The Director, CCDC, 12 Union Road, Cambridge, CB2 1EZ, UK. Fax: +44(1223)336-033, e-mail: deposit@ccdc.cam.ac.uk, or www: www.ccdc.cam.ac.uk. The cif files for the structures determined more than once (e.g. 1a, 1b, 1c1) are available on request form the Authors (MK, AO, MB)

Acknowledgements

This work was carried out in partial fulfillment of the requirements for the M.Sc. theses of Mr M.B. and carried out in both Universities of Ioannina-Greece and A. Mickiewicz-Poland within the framework of the ERASMUS program. A.M.O is a scholar of the project “Scholarship support for Ph.D. students specializing in majors strategic for Wielkopolska’s development”, sub-measure 8.2.2 Human Capital Operational Programme, co-financed by European Union under the European Social Fund. A.M.O is also supported by the Adam Mickiewicz Fundation during the academic year 2013/2014 which is acknowledged. S.K.H. would like to thank the Unit of Environmental, Organic and Biochemical high resolution analysis-ORBITRAP-LC-MS of the University of Ioannina for providing access to the facilities.

References

[1] (a) P.D. Boyle, S.M. Godfrey, *Coord. Chem. Rev.* **2001**, *223*, 265–299; (b) P. Deplano, J.R. Ferraro, M.L. Mercuri, E.F. Trogu, *Coord. Chem. Rev.* **1999**, *188*, 71–95.

[2] (a) G.J. Corban, S.K. Hadjikakou, A.C. Tsipis, M. Kubicki, T. Bakas, N. Hadjiliadis, *New J. Chem.* **2011**, *35*, 213-224; (b) V. S.K. Daga, Hadjikakou, N. Hadjiliadis, M. Kubicki, J H.Z. dos Santos, I.S. Butler, *Eur. J. Inorg. Chem.* **2002**, 1718-1728; (c) C.D. Antoniadis, G. Corban, S.K. Hadjikakou, N. Hadjiliadis, M. Kubicki, S. Warner, I.S. Butler, *Eur. J. Inorg Chem.* **2003**, 1635-1640; (d) C.D. Antoniadis, S.K. Hadjikakou, N. Hadjiliadis, M. Kubicki, I.S. Butler, *Eur. J. Inorg Chem.* **2004**, 4324-4329; (e) C.D. Antoniadis, S.K. Hadjikakou, N. Hadjiliadis, M. Kubicki, I.S. Butler, *New J. Chem.* **2005**, *29*, 714 – 720; (f) G.J. Corban, S.K. Hadjikakou, N. Hadjiliadis, M. Kubicki, E.R.T. Tiekink, I.S. Butler, E. Drougas, A.M. Kosmas, *Inorg. Chem.* **2005**, *44*, 8617-8627; (g) C.D. Antoniadis, S.K. Hadjikakou, N. Hadjiliadis, A. Papakyriakou, M. Baril, I.S. Butler, *Chem. Eur. J.* **2006**, *12*, 6888 – 6897; (h) S.K. Hadjikakou, N. Hadjiliadis, *Bioinorganic Chemistry and Applications* **2006**, *Article ID 60291*, Pages 1–10; (i) I.-E. Parigoridi, G.J. Corban, S.K. Hadjikakou, N. Hadjiliadis, N. Kourkoumelis, G. Kostakis, V. Psycharis, C.P. Raptopoulou, M. Kubicki, *Dalton Trans.* **2008**, 5159–5165; (j) A.M. Owczarzak, M. Kubicki, N. Kourkoumelis, S.K. Hadjikakou, *RSC Advances.* **2012**, *2*, 2856-2867; (k) G.J. Corban, C.D. Antoniadis, S.K. Hadjikakou, N. Kourkoumelis, V.Yu. Tyurin, A. Dolgano, E.R. Milaeva, M. Kubicki, P. V. Bernhardt, E.R.T. Tiekink, S. Skoulika, N. Hadjiliadis, *Heteroatom Chemistry* **2012**, *23*, 498-511. (l) J.H.Z. dos Santos, I.S. Butler, V. Daga, S.K. Hadjikakou, N. Hadjiliadis, Spectrochim. Acta Part A 58 (2002) 2725–2735

[3] P.D. Boyle, J. Christie, T. Dyer, S.M. Godfrey, I.R. Howson, C. McArthur, B. Omar, R.G. Pritchard, G.R. Williams, *J. Chem. Soc., Dalton Trans.* **2000**, 3106-3112.

[4] (a) F. Bigoli, P. Deplano, A. Ienco, C. Mealli, M.L. Mercuri, M.A. Pellinghelli, G. Pintus, G. Saba, E.F. Trogu, *Inorg. Chem.* **1999**, *38*, 4626–4636; (b) F. Bigoli, P. Deplano, M.L.

Mercuri, M.A. Pellinghelli, A. Sabatini, E.F. Trogu, A. Vacca, *J. Chem. Soc., Dalton Trans.* **1996**, 3583–3598; (c) D. Arzei, P. Deplano, E.F. Trogu, F. Bigou, M.A. Pellinghelli, A. Vacca, *Can. J. Chem.* **1988**, *66*, 1483–1489; (d) F. Cristiani, F.A. Devillanova, A. Diaz, G. Verani, *J. Chem. Soc., Perkin Trans.* **1984**, *2*, 1383–1386; (e) F.A. Devillanova, G. Verani, *Tetrahedron* **1979**, *35*, 511–514; (f) M.C. Aragoni, M. Arca, F. Demartin, F.A. Devillanova, A. Garau, F. Isaia, V. Lippolis, G. Verani, *J. Am. Chem. Soc.* **2002**, *124*, 4538–4539; (g) P. Deplano, F.A. Devillanova, J.R. Ferraro, F. Isaia, V. Lippolis, M.L. Mercuri, *Appl. Spectrosc.* **1992**, *46*, 1625–1629; (h) M.C. Aragoni, M. Arca, M.B. Carrea, F. Demartin, F.A. Devillanova, A. Garau, F. Isaia, V. Lippolis, G. Verani, *Eur. J. Inorg.Chem.* **2004**, *23*, 4660–4668.

[5] F. Freeman, J.W. Ziller, H.N. Po, M.C. Keindl, *J. Am. Chem. Soc.* **1988**, *110*, 2586–2591.

[6] P.H. Svensson, L. Kloo, *Chem. Rev.* **2003**, *103*, 1649–1684.

[7] W.W. du Mont, G. Mugesh, C. Wismach, P.G. Jones, *Angew. Chem., Int. Ed.* **2001**, *40*, 2486–2489.

[8] W.T. Pennington, T.W. Hanks, H.D. Arman, *Struct. Bonding* **2008**, *126*, 65–104.

[9] C. Ouvrard, J.-Y. Le, Questel, M. Berthelot, C. Laurence, *Acta Crystallogr.,* **2003**, *B59*, 512–526.

[10] D.W. Allen, R. Berridge, N. Bricklebank, S.D. Forder, F. Palacio, S.J. Coles, M.B. Hursthouse, P.J. Skabara, *Inorg. Chem.* **2003**, *42*, 3975-3977.

[11] (a) Q. Li, R. Li, Z. Zhou, W. Li, J. Cheng, *J. Chem. Phys.* **2012**, *136*, 14302; (b) P.J. Skabara, *Annu. Rep. Prog. Chem., Sec. A* **2002**, *98*, 93-105.

[12] L.C. King, I. Ryden, *J. Am. Chem. Soc.* **1947**, *69*, 1813-1814.

[13] M.A. Metwally, E. Abdel-Latif, F.A. Amer, G. Kaupp, *J. Sulfur Chem.* **2004**, *25*, 63-85.

[14] (a) A. Kleemann, J. Engel, *Pharmaceutical Substances, 4th Edition* (**2001**); (b) B.A. Baviskar, S.S. Khadabadi, S.L. Deore, *Journal of Chemistry* **2013**, art. no. 656271; (c) S.M. Basavarajaiah, B.H.M. Mruthyunjayaswamy, *Indian J. Chem.* **2010**, *49B*, 1117-1126; (d) N.J.

Thumar, M.P. Patel, *Arch. Pharm. Chem. Life Soc.*, **2011**, *2*, 91-101; (e) G.N. Sasidharan, K. Mohanan, A.N. Lakshim-Prabha, *Asian J. Chem.* **2002**, *14*, 1545-1550; (f) A. B. Nadkarni, R. V. Kamath, G. B. Khadse, *Indian J. Heterocyclic Chem.* **2000**, *9*, 309; (g) K.A. Karpov, B.V. Pekarevskii, V.M. Potekhin, *Russ. J. Gen. Chem.* **2001**, *79*, 1484-1486; (h) M. Lang, M.H.-J. Seifert, K.K. Wolf, A. Aschenbrenner, R. Baumgartner, T. Wieber, V. Trentinaglia, M. Blisse, N. Tajima, T. Yamashita, D. Vitt, H. Noda, *Bioorg. Med. Chem. Lett.* **2011**, *21*, 5417-5422.

[15] (a) F.M. Awadallah, *Sci. Pharm.* **2008**, *76*, 415-438; (b) S. Ueda, H. Terauchi, M. Kawasaki, A. Yano, M. Ido, *Chem. Pharm. Bull.* **2004**, *52*, 634-637; (c) D.G. Craciunescu, A. Furlani, V. Scarcia, A. Doadrio, *Biol. Trac. Elem. Res.* **1985**, *8*, 251-261; (d) V.A. Morde, M.S. Shaikh, R.R.S. Pissurlenkar, E.C. Coutinho, *Mol. Divers.* **2009**, *13*, 501-517; (e) S.R. Pattan, V.V.K. Reddy, P.D. Pawar, N.S. Desai, A.R. Bhat, A.D. Taranalli, *Orig. Res. Articles* **2006**, *8*, 253; (f) M. Ohkubo, A. Kuno, I. Nakanishi, H. Takasugi, *Chem. Pharm. Bull.* **1995**, *43*, 1497; (g) S.R. Pattan, V.V.K. Reddy, F.V. Manvi, B.G. Desai, A.R. Bhat, *Indian J. Chem.* **2006**, *45B*, 1778-1781; (h) G.M. Dubowchik, J.A. Michne, D. Zuev, W. Schwartz, P.M. Scola, C.A. James, E.H. Ruediger, S.S. Pin, K.D. Burris, L.A. Balanda, Q. Gao, D. Wu, L. Fung, T. Fiedler, K.E. Browman, M.T. Taber, J. Zhang, *Bioorg. Med. Chem. Lett.* **2003**, *13*, 3997-4000.

[16] (a) V.S. Ashalekshmi, K. Mohnan, *Asian J. Chem.* **2008**, *20*, 623-628; (b) Y. Sindhu, C.J. Athira, M.S. Sujamol, K. Mohnan, *Phos. Sulf. Silicon* **2010**, *185*, 1955-1963; (c) M. Bröring, C. Kleeberg, *Inorg. Chim. Acta* **2007**, *360*, 3281-3286.

[17] (a) K. Singh, S. Singh, J.A. Taylor, *Dyes Pigm.* **2002**, *54*, 189-200; (b) M. She, Z. Yang, B. Yin, J. Zhang, J. Gu, W. Yin, J. Li, G. Zhao, Z. Shi, *Dyes Pigm.* **2012**, *92*, 1337-1343; (c) X.-L. He, Y.-Q. Wang, K.-Q. Ling, *Talanta* **2007**, *72*, 747-754; (d) K.A. Karpov, A.V. Nazarenko, B.V. Pekarvskii, V.M. Potekhin, *Russ. J. Appl. Chem.* **2001**, *74*, 998-1001. e) L.N. Rasina, O.N. Chupakhin, *Radioekologiya* **1999**, *39*, 223–226.

[18] (a) A. Castro, T. Castaño, A. Encinas, W. Porcal, C. Gil, *Bioorg. Med. Chem. Lett.* **2006**, *14*, 1644-1652; (b) L. Florani, C. Boga, *J. Chem. Soc., Perkin Trans. 2*, **2002**, 768-772.

[19] (a) Y. Kohara, K. Kubo, E. Imamiya, T. Wada, Y. Inada, T. Naka., *J. Med. Chem.* **1996**, *39*, 5228-5235; (b) U.K.M. Decking, M. Hartmann, *J. Naunyn-Schmiedeberg's Arch. Pharm.* **1998**, *358*, 547-553; (c) M. Hartmann, U.K.M. Decking, *J. Naunyn-Schmiedeberg's Arch. Pharm.* **1998**, *358*, 554-560; (d) A. Lanzafame, A. Christopoulos, *J. Pharmacol. Exp. Ther.* **2004**, *308*, 830-837; (e) T.F. Tam, R. Leung-Toung, W. Li, M. Spino, K. Karimian, *Mini Rev. Med. Chem.* **2005**, *5*, 367; (f) J. Marcinkieviciene, M.J. Rogers, L. Kopcho, W. Jiang, K.Wang, D.J. Murphy, J. Lippy, S.Link, T.D.Y. Chung, F. Hobbs, T. Haque, G.L. Trainor, A. Slee, A.M. Stern, R. Copeland, *Biochem. Pharmacol.* **2000**, *60*, 339-342; (g) Y. Song, D.T. Connor, A.D. Sercel, R.J. Sorenson, R. Doubleday, P.C. Unangst, B.D. Roth, V.G. Beylin, R.B. Gilbersten. K. Chan, D.J. Schrier, A. Guglietta, D.A. Bornemeier, *J. Med. Chem.* **1999**, *42*, 1161-1169; (h) Y. Iizawa, K. Okonogi, R. Hayashi, T. Iwahi, T. Yamazaki, A. Imada, *Antimicrob. Agents Chemotherap.* **1993**, *37*, 100-105; (i) A. Martinez, M. Alonso, A. Castro, C. Pèrez, F.J. Moreno, *J. Med. Chem.* **2002**, *45*, 1292-1299.

[20] (a) T.B. Johnson, C.O. Edens, *J. Am. Chem. Soc.* **1942**, *64*, 2706-2708; (b) F.H. Herbstein, W. Schwotzert, *J. Am. Chem. Soc.* **1984**, *106*, 2367-2373.

[21] C. Laurence, M.J. El Ghomari, J-Y, Le Questel, M, Berthelot, R. Mokhlisse, *J. Chem. Soc., Perkin Trans.* **1998**, *2*, 1545-1551.

[22] (a) O. Foss, J. Johnsen, O. Tvedten, *Acta Chem. Scand.* **1958**, *12*, 1782-1798. (b) T. Lis, P. Starynowicz, Acta Cryst. C41, 1985, 1299-1302

[23] (a) D. Jiao, M. Barfield, J.E. Combariza, V.J. Hruby, *J. Am. Chem. Soc.* **1992**, *114*, 3639-3643; (b) W.-K. Li, S.-W. Chiu, Z.-X. Ma, C.-L. Liao, C.-Y. Ng, *J. Chem. Phys.* **1993**, *19*, 8440-8444; (c) M.F. Erben, C.O. Della Védova, *Helv. Chim. Acta* **2003**, *86*, 2379-2395.

[24] N.R. Kuncher, M.R. Truter, *J. Chem. Soc.* **1958**, 2551-2557.

[25] (a) M. Hołyńska, M. Korabik, M. Kubiak, *Polyhedron*, **2010**, *29*, 530-538; (b) M. Hołyńska,

M. Kubiak, Acta Cryst. 2008, C64, o609-o612.

[26] J. Coetzee, S. Cronje, L. Dobrzańska, H.G. Raubenheimer, G. Jooné, M.J. Nellb, H.C. Hoppe, *Dalton Trans.* **2011**, *40*, 1471-1483.

[27] (a) S.J. Rettig, J. Trotter, *Acta Crystallogr.* **1987**, *C43*, 2260; (b) A.C. Gallacher, A.A. Pinkerton, *Acta Crystallogr.* **1993**, *C49*, 125; (c) M. Bolte, *Private Communication* **2005**; (d) L.M. Goldsmith, C.E. Strouse, *J. Am. Chem. Soc.* **1977**, *99*, 7580.

[28] (a) A. Altomare, G. Cascarano, C. Giacovazzo, A. Gualardi, *J.Appl. Cryst.* **1993**, *26*, 343-350; (b) C.K. Johnson, *ORTEPII. Report ORNL-5138*. Oak Ridge National Laboratory, Tennessee, USA (**1976**). (c) C.F. Macrae, I.J. Bruno, J.A. Chisholm, P.R., Edgington, P. McCabe, E. Pidcock, L. Rodriguez-Monge, R. Taylor, J. van de Streek, P.A. Wood, *J. Appl. Cryst.* **2008**, *41*, 466–470.

Figure Captions

Figure 1 Conductivity titration of TU or MeTU (10^{-2} M) with I_2 in acetonitrile (T= 293 K).

Figure 2 (**A**) UV spectra of TU and its complexes **1-4** in dichloromethane (4.3 10^{-4} M (**TU**), 2.0 10^{-4} M (**1a, 1c**), 2.9 10^{-4} M (**1b**), 7.0 10^{-4} M (**2**), 6.1 10^{-4} M (**3**), 3.1 10^{-4} M (**4**)). (**B**) UV spectra of MeTU and its the complexes **5-6** in dichloromethane..

Figure 3 **(A)** ORTEP diagram together with atomic numbering scheme of **1.** Thermal ellipsoids drawn at the 75% probability level, hydrogen atoms are represented by spheres of arbitrary radii. Thin lines represent hydrogen bonds. The unlabeled part of the cation is related with the labeled one by symmetry operation *3/2-x,3/2-y,z*. (**B**) Hydrogen bonds and S···S interactions in the crystal structure of **1**.

Figure 4 (**A**) ORTEP diagram together with atomic numbering scheme of **2**. Thermal ellipsoids drawn at the 50% probability level. hydrogen atoms are represented by spheres of arbitrary radii. Thin lines represent hydrogen bonds. The unlabeled part of the triodide is related with the labeled one by symmetry operation *1-x, -y1-,z*. (**B**). Packing along *y* direction in **2** with hydrogen bonds.

Figure 5 (**A**) ORTEP diagram together with atomic numbering scheme of **3**. Thermal ellipsoids drawn at the 75% probability level, hydrogen atoms are represented by spheres of arbitrary radii.. (**B**) Packing along *z* direction in **3** with hydrogen bonds. and S···I intermolecular interactions.

Figure 6 **(A)** ORTEP diagram together with atomic numbering scheme of **4**. Thermal ellipsoids drawn at the 50% probability level, hydrogen atoms are represented by spheres of arbitrary radii. The unlabeled iodine atoms are related with the labeled one by symmetry operations *2-x, 2-y, 1-,z* (I2) and *1-x,1-y,1-z* (I4).. (**B**) Packing diagram of **4** as seen along *y* direction; hydrogen bonds and short intermolecular contacts are drawn as dashed lines.

Figure 7 **(A)** ORTEP diagram together with atomic numbering scheme of **5**. Thermal ellipsoids drawn at the 50% probability level, hydrogen atoms are represented by spheres of arbitrary radii. Thin lines represent hydrogen bonds. The unlabeled part of the triodide is related with the labeled one by symmetry operation *-x,-y3/2-,z*.(**B**) Packing diagram of **4** as seen along *y* direction; hydrogen bonds are drawn as dashed lines.

Figure 8 **(A)** ORTEP diagram together with atomic numbering scheme of **6**, hydrogen atoms are represented by spheres of arbitrary radii.. Thermal ellipsoids drawn at the 75% probability level. (**B**) Packing diagram of **6** as seen along *y* direction; hydrogen bonds and short intermolecular contacts are drawn as dashed lines.

Figure 9 **(A)** ORTEP diagram together with atomic numbering scheme of **7**. Thermal ellipsoids drawn at the 50% probability level, hydrogen atoms are represented by spheres of arbitrary radii. Thin lines represent weaker I…I bond, dashed lines represent hydrogen bonds. The unlabeled part of the cation is related with the unlabeled one - by symmetry operation *x+1/2,y,-z+1/2* while that of tetraiodide - by *-x,-y,-,z*. (**B**) Packing diagram of **7** as seen along *y* direction; hydrogen bonds and short intermolecular contacts are drawn as dashed lines.

Figure 10 **(A)** ORTEP diagram together with atomic numbering scheme of **8**. Thermal ellipsoids drawn at the 75% probability level, hydrogen atoms are represented by spheres of arbitrary radii.. (**B**) Packing diagram of **8** as seen along *y* direction; hydrogen bonds and short intermolecular contacts are drawn as dashed lines

Figure 11 **(A)**. ORTEP diagram together with atomic numbering scheme of **9**. Thermal ellipsoids drawn at the 50% probability level, hydrogen atoms are represented by spheres of arbitrary radii.. (**B**) Packing diagram of **9** as seen along *x* direction; hydrogen bonds and short intermolecular contacts are drawn as dashed lines.

Figure 12 Relationship between S-S bond distance *vs* C-S-S-C torsion angle in compounds **1**, **2**, **4**, **5** ($y=1.18\cdot10^{-4}x^2+2.23\cdot10^{-2}x+3.07$; $R^2= 0.972$).

Table 1. Selected bond distances and angles of **1, 2, 3, 4, 5 and 7.**

complex **1**		complex **2**		complex 3		complex **4**		complex **5**		complex **7**	
bond length [Å]											
S1-S1	2.0244(14)	S1-S2	2.038(2)	S1-C1	1.739(3)	S1-S2	2.0294(19)	S1-S1	2.029(2)	S1-S1	2.011(4)
S1-C1	1.783(3)	S1-C1	1.780(6)	C1-N11	1.317(4)	S1-C1	1.759(6)	S1-C1	1.781(4)	S1-C1	1.756(7)
C1-N11	1.305(4)	S2-C2	1.778(6)	C1-N12	1.307(4)	S2-C2	1.777(6)	C1-N11	1.311(6)	C1-N11	1.299(10)
C1-N12	1.306(4)	C1-N11	1.307(8)	I1-I2	2.8558(3)	C1-N11	1.308(8)	C1-N12	1.317(5)	C1-N12	1.296(10)
		C1-N12	1.303(7)	I2-I3	2.9961(3)	C1-N12	1.286(9)			N12-C12	1.452(10)
		C2-N21	1.316(8)			C2-N21	1.313(8)			I1-I1	2.7728(16)
		C2-N22	1.300(8)			C2-N22	1.298(8)			I1-I2	3.4022(11)
		I2-I3	2.9246(4)			I1-I2	2.9220(6)				
						I3-I4	2.9172(5)				
angles [°]											
S1-S1-C1	102.75(12)	S2-S1-C1	102.7(2)	S1-C1-N11	119.1(2)	S2-S1-C1	102.8(2)	S1-S1-C1	102.93(14)	S1-S1-C1	102.4(3)
S1-C1-N11	122.0(2)	S1-S2-C2	103.2(2)	S1-C1-N12	119.6(2)	S1-S2-C2	102.4(2)	S1-C1-N11	114.3(3)	S1-C1-N11	12430(6)
S1-C1-N12	114.2(3)	S1-C1-N11	114.7(4)	N11-C1-N12	121.2(3)	S1-C1-N11	114.6(5)	S1-C1-N12	122.5(3)	S1-C1-N12	112.9(6)
N11-C1-N12	123.7(3)	S1-C1-N12	122.7(5)	I1-I2-I3	179.102(9)	S1-C1-N12	123.0(5)	N11-C1-N12	123.2(4)	N11-C1-N12	123.1(7)
		S2-C2-N21	122.6(5)			S2-C2-N21	123.1(4)			C1-N12-C12	124.1(7)
		S2-C2-N22	114.6(5)			S2-C2-N22	114.8(5)			I1-I1-I2	178.46(4)
		N11-C1-N12	122.6(6)			N11-C1-N12	122.4(6)				
		N21-C2-N22	122.8(6)			N21-C2-N22	122.1(6)				
		I3-I2-I3	180			I2-I1-I2	180				
						I4-I3-I4	180				
torsions [°]											
C1-S1-S1-C1	94.1(2)	C1-S1-S2-C2	94.5(3)			C1-S1-S2-C2	102.7(3)	C1-S1-S2-C2	86.4(3)	C1-S1-S1-C1	98.0(5)
hydrogen bonds lengths [Å] and angles [°]											
N11[H]···O11W	2.950(3)	N11[H]···Cl1	3.159(5)	S1[H]···I1	3.9694(9)	N12[H]...BR1	3.305(6)	N11[H]···O1W	2.868(5)	N12[H]···Br1	3.392(7)
O1W[H]···I1	3.5231(17)	N22[H]···Cl1	3.155(5)			N21[H]...BR1	3.377(6)	O1W[H]···BR1	3.326(3)		
						N22[H]...BR1	3.409(6)	N12[H]···BR1	3.286(4)		
						N22[H]...BR1	3.436(6)	N12[H]···BR1	3.390(3)		
N11-H11B···O1W	149	N11-H11B···Cl1	164	S1-H1···I1	167	N12-H12A...BR1	162	N11-H11B···O1W	168	N12-H12···Br1	175
O1W-H1W···I1	171(4)	N22-H22B···Cl1	167			N21-H21A...BR1	153	O1W-H1W···BR1	178(5)		
						N22-H22A...BR1	152	N12-H12A···BR1	162		
						N22-H22B...BR1	166	N12-H12B···BR1	141		
close contacts [Å]											
S1···S1	3.481(2)	S1···Cl1	3.374(2)	S1···I1	3.7689(8)	S1···S2	3.572(2)	S1···O1W	3.320(1)	S1···I2	3.645(2)
		S2···Cl1	3.423(2)					C1···BR1	3.578(4)		
						S1···BR1	3.496(2)				

Table 2. Selected bond distances and angles of **6**, **8** and **9**.

complex **6**		complex **8**		complex **9**	
bond lengths [Å]					
S1-N2	1.696(2)	S1-C2	1.731(3)	S1-N2	1.684(6)
S1-C5	1.744(3)	S1-C5	1.740(3)	S1-C5	1.704(7)
N2-C3	1.334(3)	C2-N3	1.341(4)	N2-C3	1.321(8)
C3-N4	1.342(3)	N3-C4	1.409(4)	C3-N4	1.398(8)
C3-N31	1.328(3)	C4-C5	1.343(5)	C3-N31	1.320(8)
N4-C5	1.327(3)	C2-N21	1.323(4)	N31-C32	1.456(8)
C5-N51	1.310(4)	N3-C31	1.469(4)	N4-C5	1.335(8)
		C4-C41	1.493(4)	N4-C41	1.481(8)
				C5-N51	1.336(8)
				I1-I2	2.9718(6)
				I2-I3	2.8710(6)
angles [º]					
N2-S1-C5	87.06(12)	C2-S1-C5	90.02(16)	N2-S1-C5	93.0(3)
S1-N2-C3	112.62(19)	S1-C2-N3	111.7(2)	S1-N2-C3	109.6(5)
N2-C3-N4	115.9(2)	C2-N3-C4	113.9(3)	N2-C3-N4	115.1(6)
C3-N4-C5	109.5(2)	N3-C4-C5	112.0(3)	C3-N4-C5	111.9(6)
S1-C5-N4	114.9(2)	S1-C5-C4	112.4(3)	S1-C5-N4	110.3(5)
N2-C3-N31	122.9(3)	S1-C2-N21	124.0(3)	N2-C3-N31	125.7(6)
N31-C3-N4	121.2(2)	N21-C2-N3	124.3(3)	N31-C3-N4	119.2(6)
N4-C5-N51	123.7(2)	C2-N3-C31	120.9(3)	C3-N31-C32	121.5(6)
S1-C5-N51	121.4(2)	C31-N3-C4	125.2(3)	C3-N4-C41	121.8(6)
		N3-C4-C41	120.2(3)	C41-N4-C5	125.8(5)
		C41-C4-C5	127.7(3)	N4-C5-N51	124.8(6)
				S1-C5-N51	125.0(6)
hydrogen bonds [Å] and angles [º]					
N31[H]···N4	2.974(3)	N21[H]···O1W	2.811(4)	N51[H]···N2	2.954(10)
N51[H]···I1	3.513(2)	N21[H]···I1	3.492(3)		
		O1W[H]···I1	3.555(3)		
		O1W[H]···I1	3.539(3)		
N31-H31B···N4	174	N21-H21A···O1W	163	N51-H51···N2	161
N51-H51B···I1	155	N21-H21B···I1	158		
		O1W-H1WA···I1	172		
		O1W-H1WB···I1	171		
close contacts					
S1···S1	3.423(1)	S1···I1	3.6421(9)	S1···I1	3.560(2)
				S1···I1[a]	3.703(2)

[a] = 1-x, 1-y, 1-z

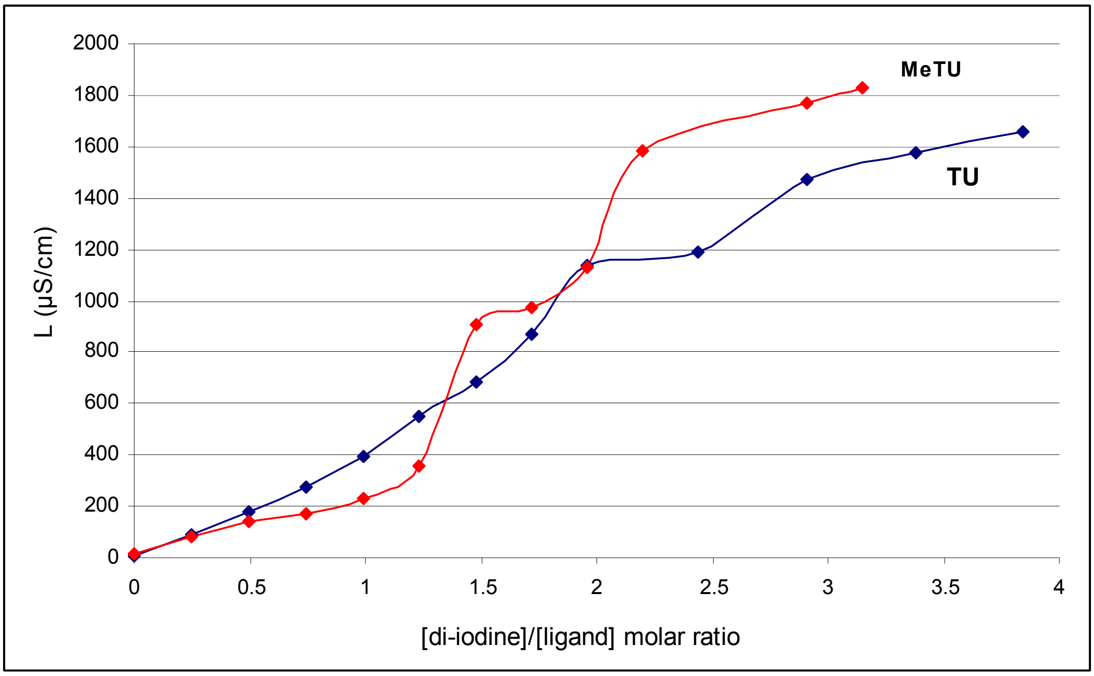
2000
1800
1600
1400
1200
1000
800
600
400
200
0
L (µS/cm)
0
0.5
1
1.5
2
2.5
3
3.5
4
[di-iodine]/[ligand] molar ratio
MeTU
TU

Figure 1

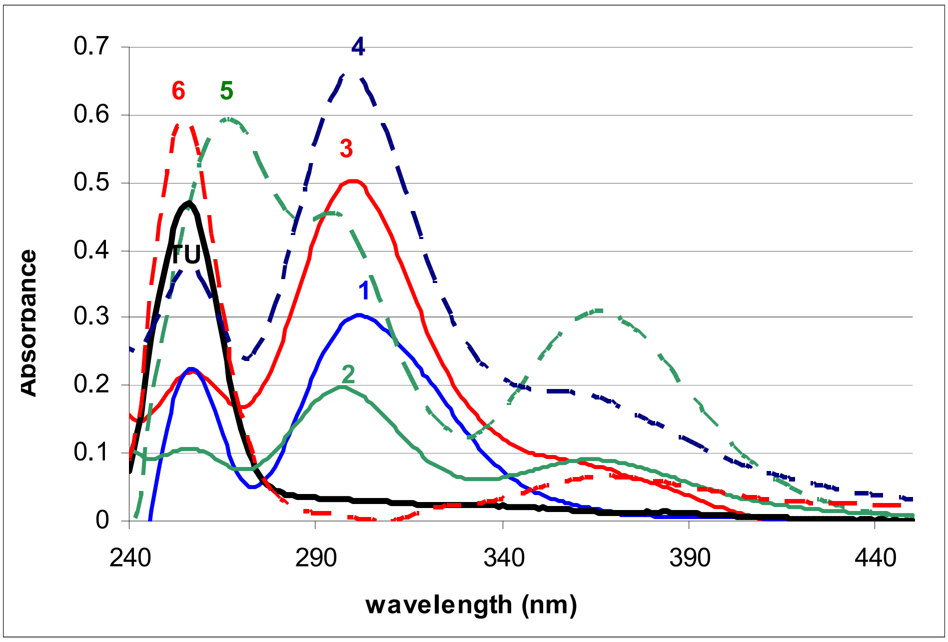
Absorbance
0.7
0.6
0.5
0.4
0.3
0.2
0.1
0
240
290
340
390
440
wavelength (nm)
4
6
5
3
TU
1
2

(A)

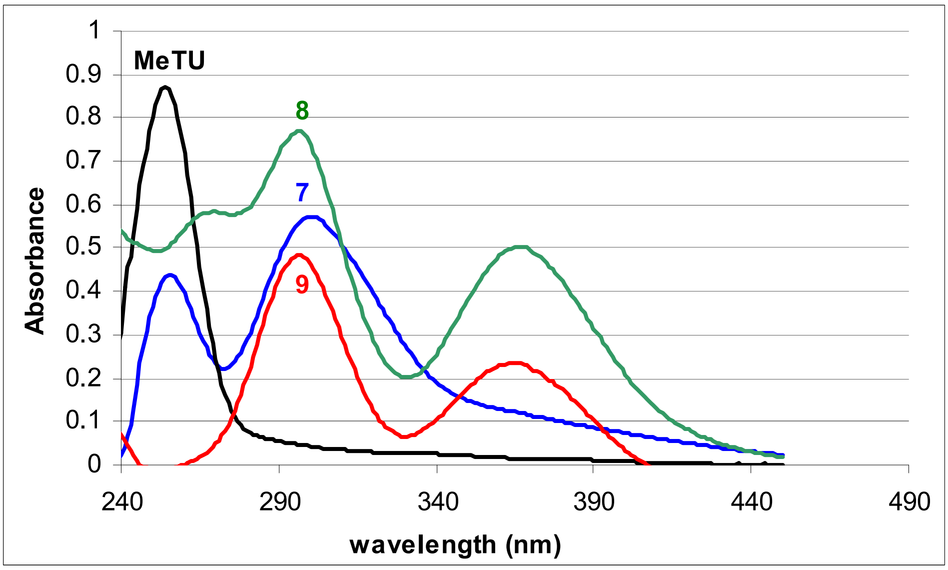
Absorbance
1
0.9
0.8
0.7
0.6
0.5
0.4
0.3
0.2
0.1
0
240
290
340
390
440
490
wavelength (nm)
MeTU
8
7
9

(B)

Figure 2

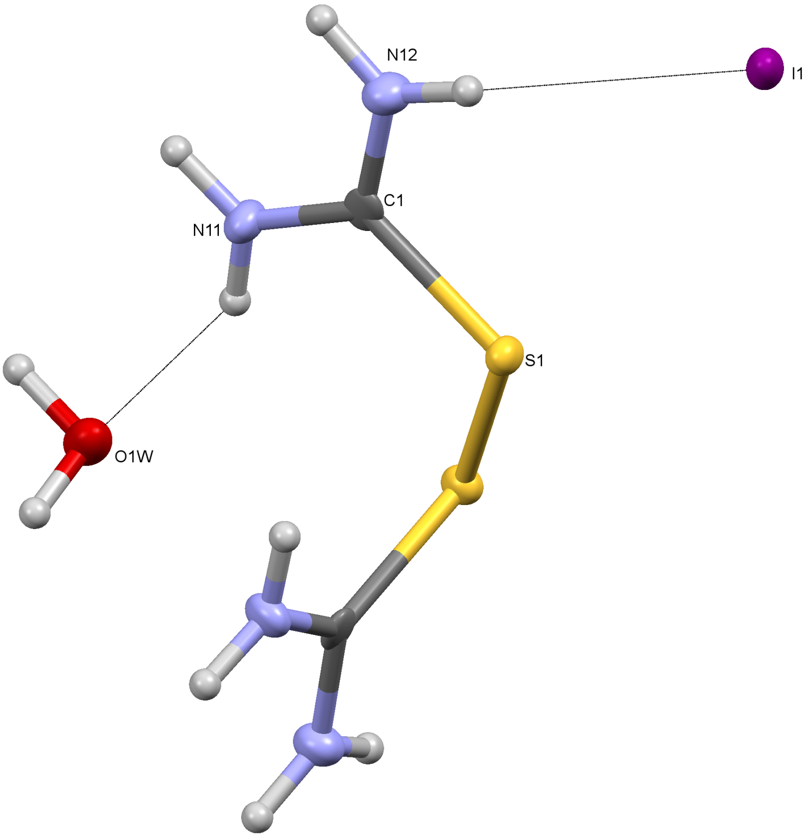

(A)

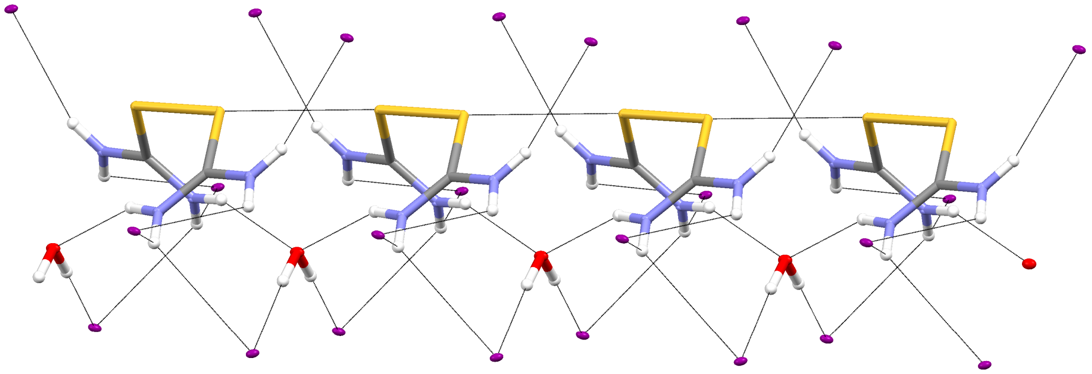

(B)

Figure 3

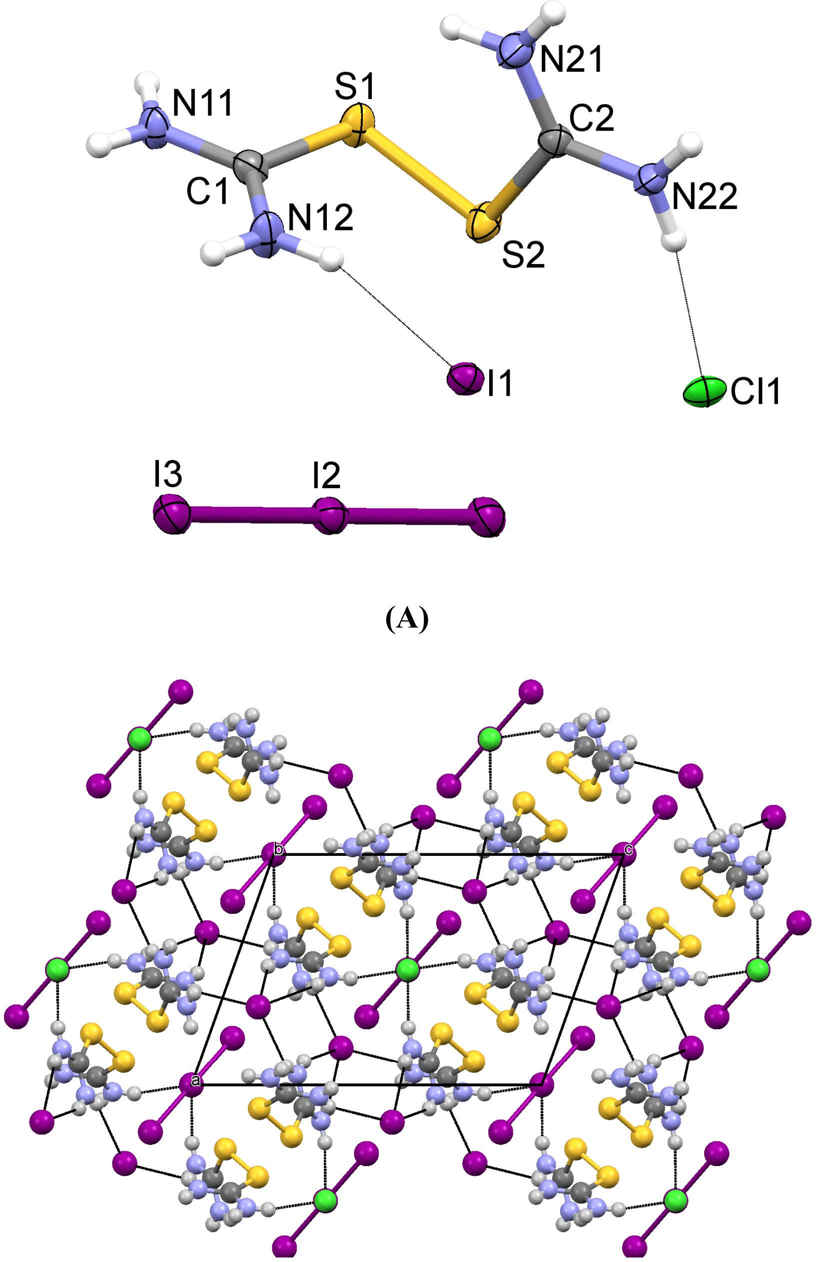

(A)

(B)

Figure 4

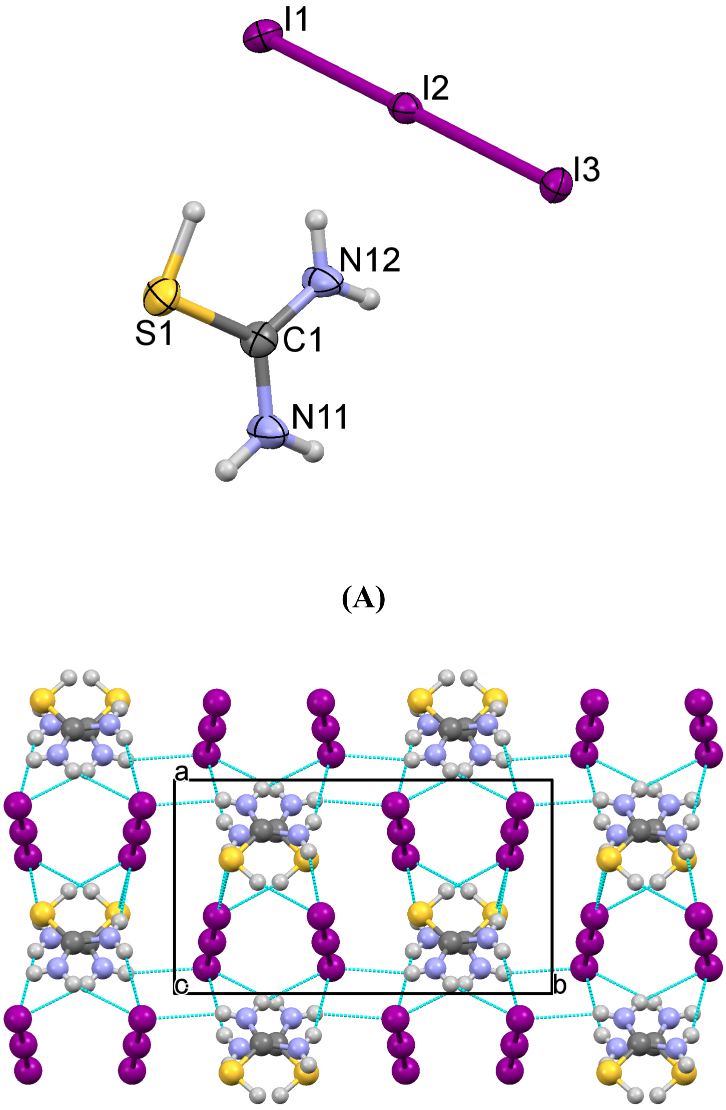

(A)

(B)

Figure 5

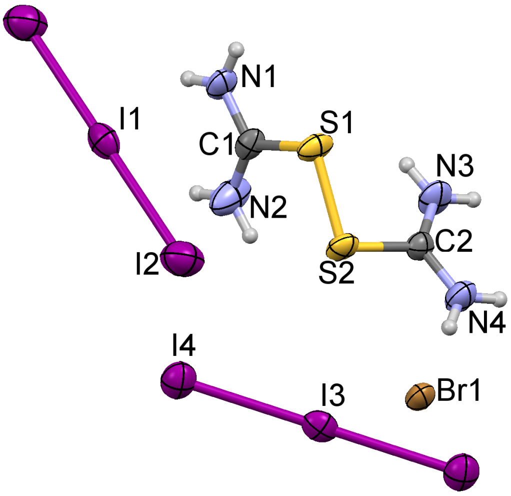

(A)

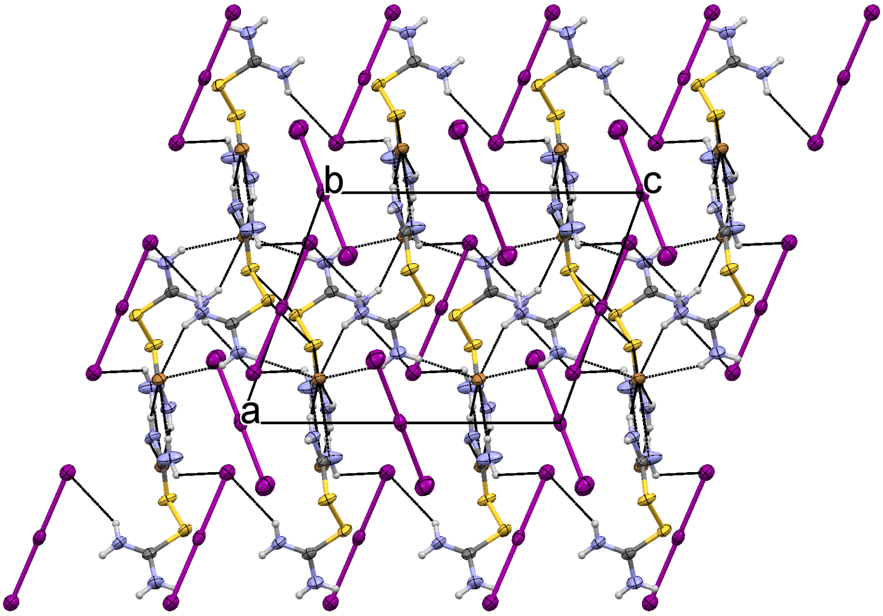

(B)

Figure 6

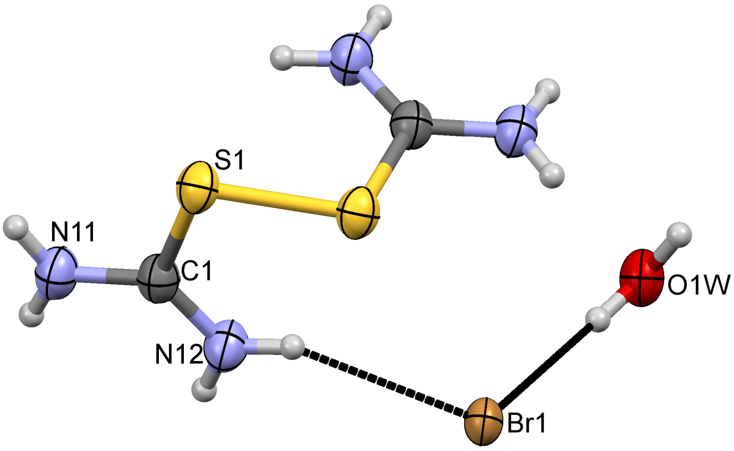

(A)

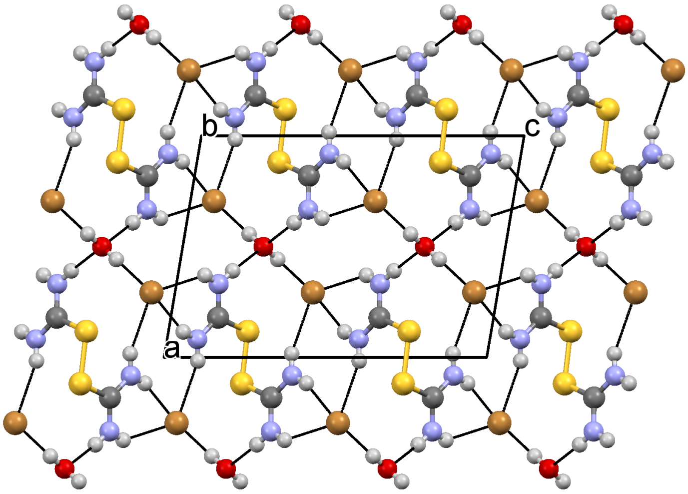

(B)

Figure 7

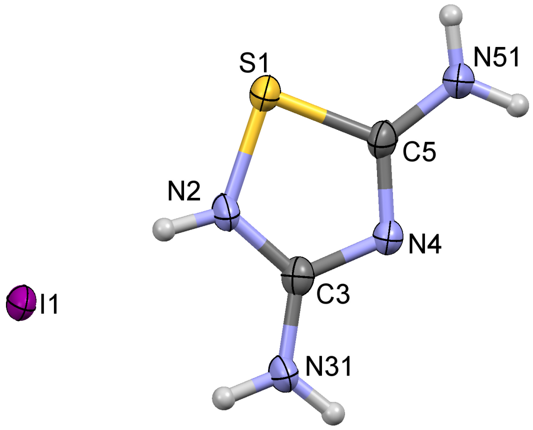

(A)

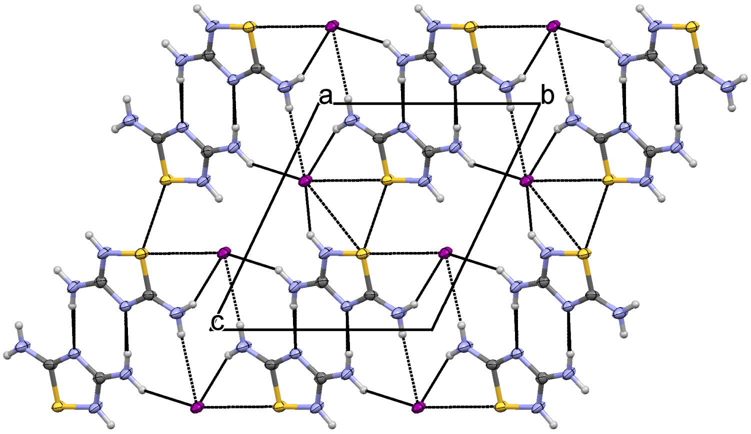

(B)

Figure 8

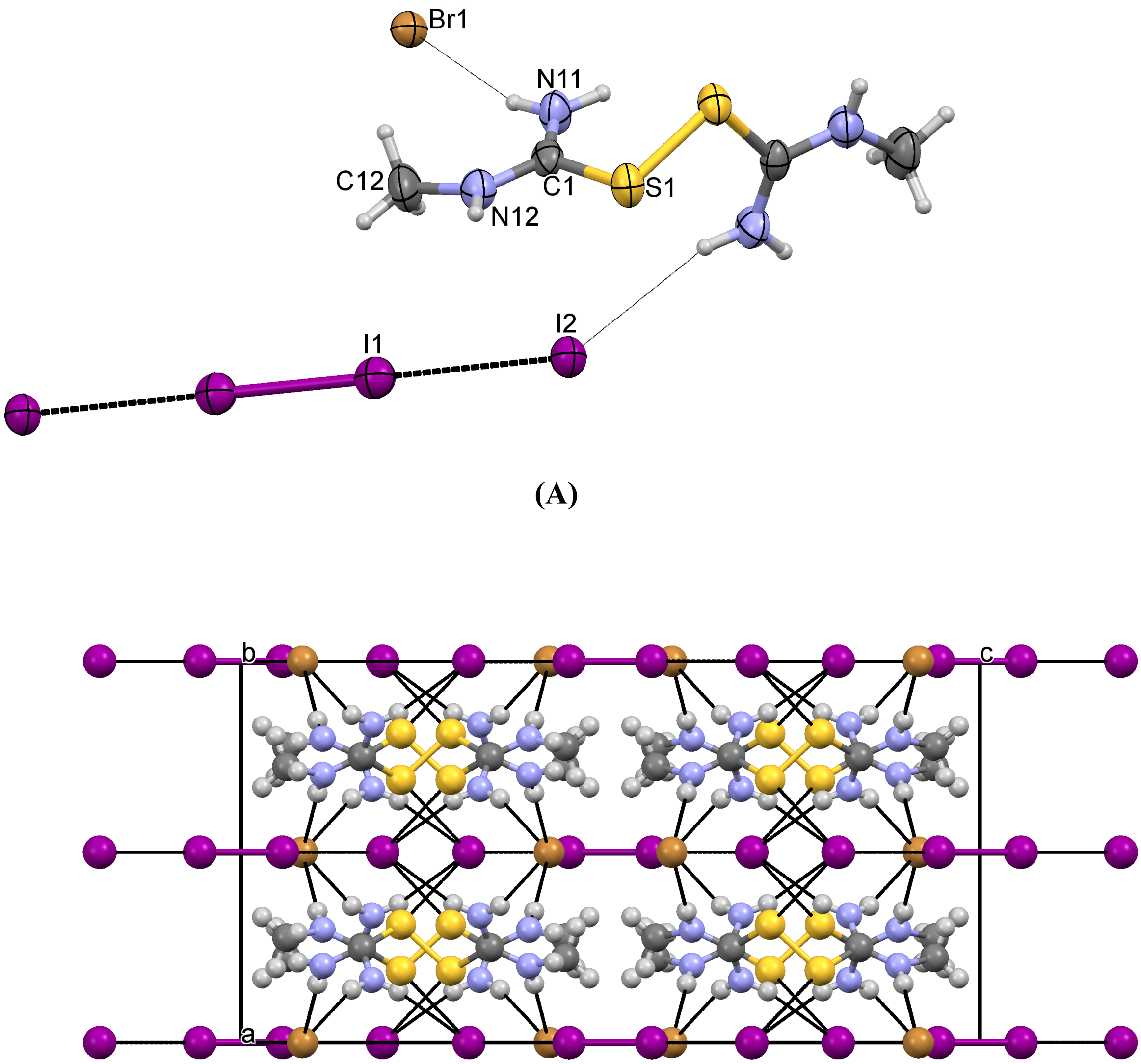

(A)

(B)

Figure 9

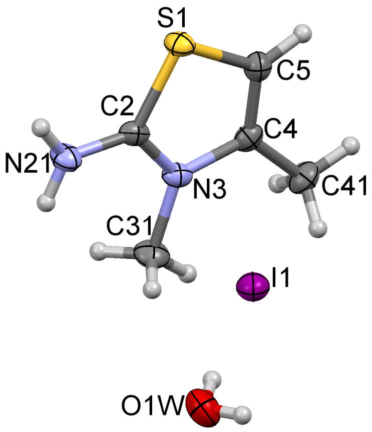

(A)

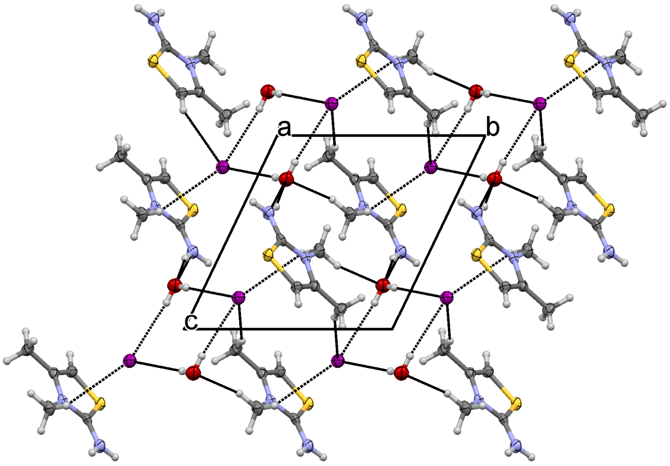

(B)

Figure 10

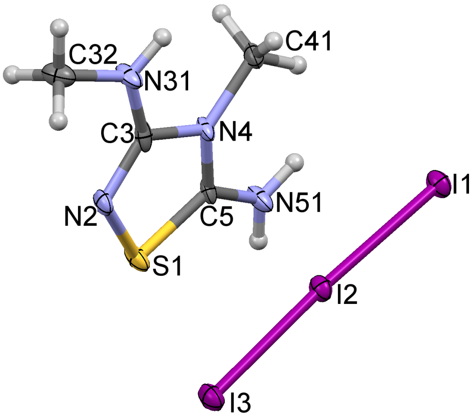

(A)

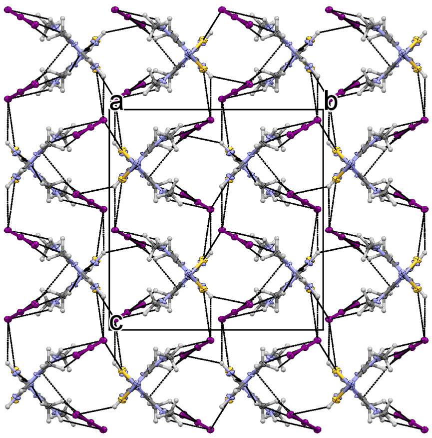

(B)

Figure 11

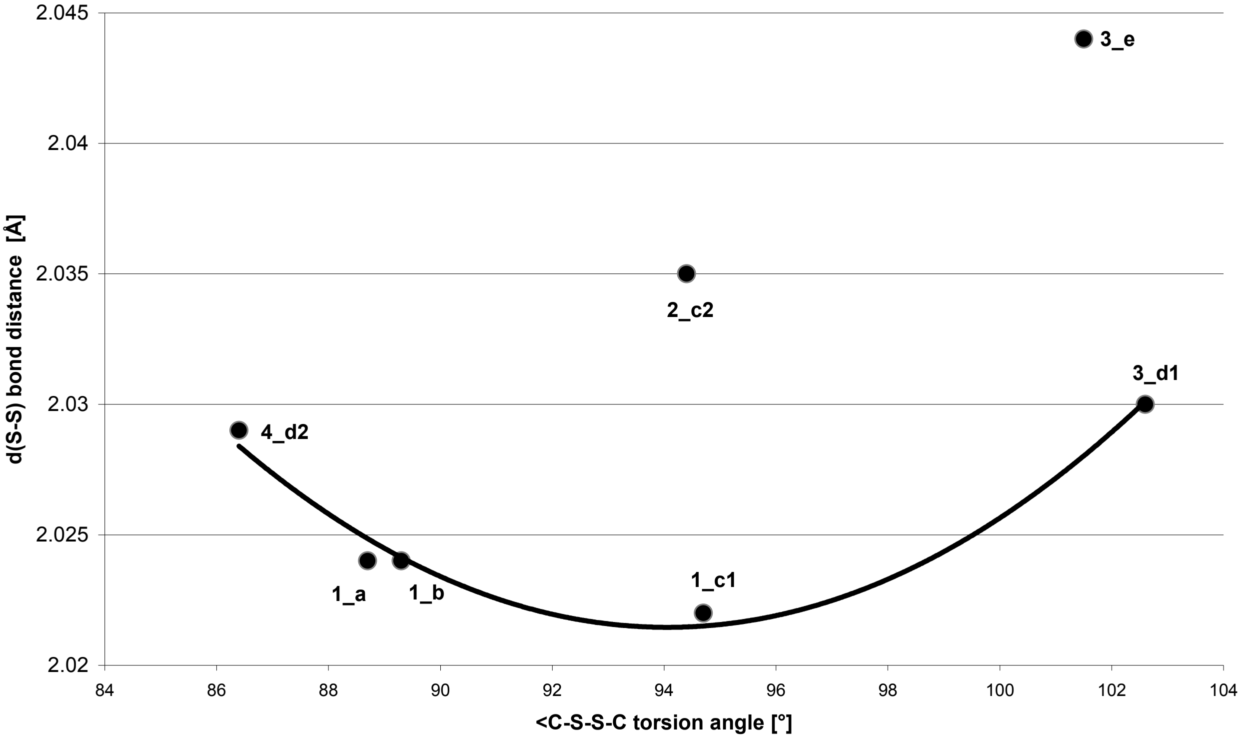
2.045
2.04
2.035
2.03
2.025
2.02
d(S-S) bond distance [Å]
84
86
88
90
92
94
96
98
100
102
104
<C-S-S-C torsion angle [°]
3_e
2_c2
3_d1
4_d2
1_a
1_b
1_c1

Figure 12